T.C.

ISTANBUL MEDIPOL UNIVERSITY

INSTITUTE OF

HEALTH SCIENCES

MASTER THESIS

EFFECT OF TRASTUZUMAB AND LONIDAMINE-LOADED LIPID NANOPARTICLES ON HER2+ BREAST CANCER

FATMA ÖZLEM ZURNACI

DEPARTMENT OF MOLECULAR MEDICINE AND BIOTECHNOLOGY

THESIS ADVISOR

Assoc. Prof. MUSTAFA GÜZEL

ISTANBUL-2021

1. ABSTRACT

EFFECT OF TRASTUZUMAB AND LONIDAMINE-LOADED LIPID NANOPARTICLES ON HER+ BREAST CANCER

Our study includes inhibition of glycolysis with HK2 target and inhibition of HER2 pathway, which is highly expressed in many cancer types, with HER2 target. Reduced survival, negative metastasis, and induced apoptosis are expected due to the combined inhibition of these two targets. Trastuzumab was used as the HER2 inhibitor, while lonidamine was used as the HK2 inhibitor. Trastuzumab is an antibody designed to selectively bind to an antigen called human epidermal growth factor 2 (HER2). Lonidamine is a derivative of indazole-3-carboxylic acid, which is known to inhibit aerobic glycolysis in cancer cells. Lonidamine was delivered to cells in hybrid nanoparticles to increase the effect of lonidamine and make it target-specific. The combination of trastuzumab and Lonidamine-loaded hybrid nanoparticles yielded positive results. Increased apoptosis in SKBR3 cells was demonstrated by Annexin V, DNA fragmentation analysis, and gene-level BAX/BCL-2 ratio. In addition, increased VDAC expression in the combination group was detected by western blot analysis. The effect of the combination of trastuzumab and lonidamine loaded nanoparticles on metastasis was determined by scratch assay and MMP-2 gene expression analyses. According to the results, the combination group gave a high significance wound area compared to all other groups. In addition, MMP-2 gene expression showed significant inhibition in the combination group compared to the control. According to our results, the combination of trastuzumab and lonidamine-loaded hybrid nanoparticles created a synergistic effect. With this combined therapy, drug resistance can be prevented. It may also be beneficial to the chemotherapy process in HER2-positive breast cancer.

Key words; Apoptosis, Lonidamine, Metastasis, Nanoparticle, Trastuzumab

2. ÖZET

TRASTUZUMAB VE LONİDAMİN YÜKLÜ LİPİD NANOPARTİKÜLLERİN HER2+ MEME KANSERİ ÜZERİNDEKİ ETKİSİ

Çalışmamız HK2 hedefiyle glikolizin inhibisyonu ve HER2 hedefiyle birçok kanser türünde yüksek ifade edilen HER2 yolağının inhibisyonunu içermektedir. Bu iki hedefin kombine inhibisyonu dolasıyla azalmış sağkalım, negatif metastaz ve indüklenmiş apoptoz beklenmektedir. Trastuzumab HER2 inhibitörü olarak kullanılırken, lonidamin HK2 inhibitörü olarak kullanıldı. Trastuzumab insan epidermal büyüme faktörü 2 (HER2) olarak adlandırılan antijene seçici olarak bağlanmak üzere tasarlanmış bir antikordur. Lonidamin kanser hücrelerinde aerobik glikolizi inhibe ettiği bilinen indazol-3-karboksilik asidin bir türevidir. Lonidaminin etkisini arttırmak ve hedef spesifik hale getirmek için Lonidamin hibrit nanopartiküller içerisinde hücrelere gönderildi. Trastuzumab ve Lonidamin yüklü hibrit nanopartiküllerin kombinasyonu pozitif sonuçlar verdi. SKBR3 hücrelerinde artmış apoptoz Annexin V, DNA fragmentasyon analizi ve gen seviyesinde BAX/BCL-2 oranı ile gösterilmiştir. Ayrıca kombinasyon grubunda artmış VDAC ekspresyonu western blot analizi ile tespit edilmiştir. Trastuzumab ve Lonidamin yüklü nanopartiküllerin kombinasyonunun metastaz üzerindeki etkisi çizik deneyi ve MMP-2 gen ekspresyonu analizleri ile tesbit edilmiştir. Sonuçlara göre kombinasyon grubu diğer tüm gruplara kıyasla yüksek anlamlı boşluk alanı vermiştir. Ayrıca MMP-2 gen ekspresyonu kombinasyon grubunda kontrole kıyasla anlamlı inhibisyon göstermiştir. Sonuçlarımıza göre Trastuzumab ve Lonidamin yüklü hibrit nanopartiküllerin kombinasyonu sinerjik etki meydana getirmiştir. Bu kombine terapi ile ilaç direncinin önüne geçilebilir. Ayrıca HER2 pozitif meme kanserinde kemoterapi sürecine faydalı olabilir.

Anahtar kelimeler; Apoptoz, Lonidamin, Metastaz, Nanopartikül, Trastuzumab

3. INTRODUCTION AND PURPOSE

The main purpose of the thesis is to determine the combined drugs that can be used in HER2-positive breast cancer and to conduct in vitro efficiency studies. For this purpose, we think that co-administration of LND and Tmab and its delivery to the target in liposomal nanoparticles will provide a great advantage both by inhibiting HK-2 and taking advantage of the effectiveness of a protein-structured drug such as Tmab. Similarly, inhibition of the HER2 pathway specifically overexpressed in breast cancer in combination with a non-toxic dose of LND provides an alternative therapy. Moreover, inhibition of both the HK2 and HER2 pathways would abolish the repression of apoptosis. With LND, we aim to induce apoptosis by hitting a barrier to the energy metabolism of cancer cells.

The drug delivery system loaded with trastuzumab and lonidamine, which we targeted in our study, has many advantages. The major benefit of combination drug therapies is that they reduce the development of drug resistance because a pathogen or tumor is less likely to become resistant to more than one drug at a time. In addition, sending drugs combined with the liposomal drug delivery system will increase the effect. Therefore, we hope to reduce drug resistance and achieve a synergistic effect by targeting both pathways in HER2-positive breast cancer.

4. LITERATURE REVİEW

Breast cancer is the most common type of cancer among women in the world and has the highest mortality rate. New cases exceeded two million in 2018, although prognosis and survival rates for breast cancer have improved significantly(1). Unlike the standard pathological features of cancers, breast cancer displays a heterogeneous disease course with various biological and morphological features. These heterogeneous structures of breast cancer make the treatment method difficult and unexpected results may occur (2). In this context, tumor classifications are needed to strongly predict clinical outcomes (3). When classifying breast cancer, 3 different receptors are evaluated; estrogen receptor (ER), progesterone receptor (PR), and human epidermal growth factor receptor 2 (HER2). With these features of tumors, they are classified as luminal A, luminal B, HER2 positive and triple negative disease, and the importance of basing treatment decisions on internal molecular subtypes of breast cancer has been internationally recognized (4).

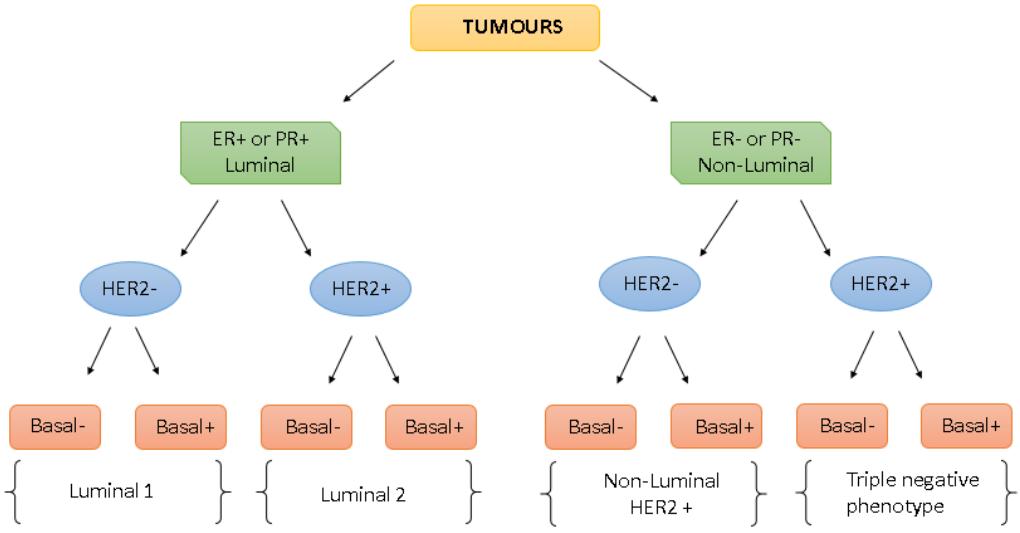


Figure 4.2. Molecular Classification of Breast Cancer Based on GeneExpression

In the vast majority of breast cancer cases, abnormalities in HER2 expression at the gene or protein level have been consociated with a contrary prognosis in both lymph node negative and lymph node positive breast cancer. In many different studies looking at approximately 40,000 patients, 88% of HER2 gene overexpression of the

HER2 protein was found to predict breast cancer outcome in univariate or too many variables analysis. (5). The obtained data suggest that HER2 overexpression is associated with an unfavorable prognosis in node-positive and node-negative breast cancer (5,6).

4.1.HER2 Receptor

The HER2 receptor (human epidermal growth factor receptor 2) is a membrane tyrosine kinase. There are 4 types of membrane receptor kinases. These; HER1 (EGFR), HER3 (erbB3) and HER4 (erbB4) are receptor tyrosine kinases. These each have a transmembrane domain(an extracellular ligand binding domain), and an intracellular tyrosine kinase catalytic domain. They are transmembrane single subunit glycoproteins(7). These receptors provide ligand activation by forming homodimers or heterodimers(8). HER2 receptors have no known ligands to make homodimers. But it can make heterodimers with all other family members. It is similar in the activated form of RTK (Receptor Tyrosine Kinase) with the structure of the extracellular domain of HER2 without bound ligand. After the activation of these receptors, other intracellular pathways are activated and transphosphorylations occur(9). These pathways are Ras / mitogen-activated protein kinase pathway (mTOR), phosphatidylinositol 3 kinase (PI3K) / Akt pathway, Janus kinase / signal converting and transcription pathway activator (JAK-STAT) and phospholipase C (PLC) pathway. As a result, many actions occur such as cell proliferation, survival, cell cycle and resistance to apoptosis (10).

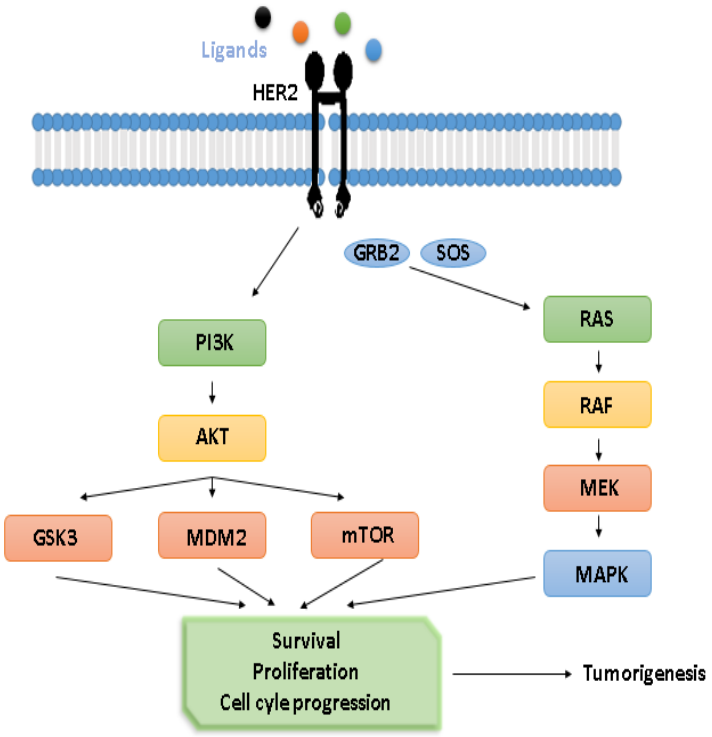


Figure 4.1.1. HER2 Receptor tyrosine kinase and its sub-pathways

HER2 oncogene is situated on chromosome 17q12(7). HER2 amplification is the first pathway of HER2 receptor overexpression and has a profound effect on tumor development and progression(11). HER2 + is overexpressed in approximately 15% to 20% of breast cancers. In this context, HER2 targeted drug studies have attracted attention for many years. In addition, various tests have been developed to determine the HER2 receptor expression level in breast cancer patients. For patients whose HER2 receptor level is determined, a different prescription is applied than other patients.

4.1.1. HER2 Expression in Primary and Metastatic Breast Cancer

HER2 overexpression is generally observed in 15% of primary breast cancers. Given the history of the disease, it has a high metastatic potential and results in decreased overall survival (5,12).

Biomarker characteristics detected in primary breast cancer may change when the tumor progresses from primary breast cancer to metastatic breast cancer(12,13).

In a retrospective study, HER2 efficiency was evaluated depending on HER2 compatibility between primary and metastatic breast cancer tissue. The transformation of HER2 amplification in the transition from primary breast cancer to metastatic breast cancer was detected in 28 of 74 cases. This transformation was mostly seen in hormone receptor-positive breast cancers. Patients with the positive change of HER2 profited significantly from first-line therapy containing HER2 inhibitors. In this series, loss of HER2 amplification produced poor treatment response in cases using anti-HER2 treatments(12).

4.1.2. HER2 Breast Cancer Expression and Histopathology

HER2 gene amplification is commonly found in the pleomorphic variant of invasive lobular carcinoma due to an negative result(14). HER2 positivity is excessively uncommon in tubular carcinoma and excessively low in mucinous (colloid) breast cancers. However, it is connected with tyson conditions(11,15).

The prognosis and management of breast carcinoma is influenced by classical variables such as histological type and grade, tumor size, lymph node status, and tumor receptor status (ER, PR, and HER2). HER2 has appeared as an important independent predictive marker in primary breast carcinoma in recent years(15).

In one study, histopathological tests were performed to investigate the relationship between the expression of ER, PR and HER2 receptors and tumor grade. According to the results obtained; This approvess that the receptor expression of ER, PR and HER2 is importantly connected with tumor grade. In addition, an opposite correlativity of HER2 expression with ER and PR expression has also been observed(16). Another study showed that higher HER2 amplification levels are connected with larger tumor size and less ER and PR expression(17).

According to the literature studies, there are many sub-pathways connectd with the HER2 receptor. Investigating these pathways and determining their roles fully will support the progression process by determining the combination of drugs to be applied in the treatment of HER2-positive breast cancer and with the right treatment(18). In this way, it is clearly seen that the positive response time will also be shortened.

4.2. HER2-Targeted Therapy

HER2-targeted therapy reversed adverse outcomes in breast and gastric cancers that overexpress HER2 receptor tyrosine kinase(19). HER2-targeted therapy is used in high rates of breast cancer. There are some approved treatments for adjuvant (post-surgical) and metastatic HER2-positive breast cancers. Pertuzumab (metastatic and adjuvant), Trastuzumab (metastatic and adjuvant), lapatinib (metastatic), ado-trastuzumab emtansine (metastatic) and neratinib (adjuvant), in addition to these, cisplatin and a fluoropyrimidine (capecitabine or 5-fluorouracil) are used(20,21). These treatments are also sanctioned for other HER2-positive cancer types. In addition to these treatments, Trastuzumab-dkst (Ogivri; Mylan) has been approved as a trastuzumab biosimilar and is used in the chemotherapy process(21).

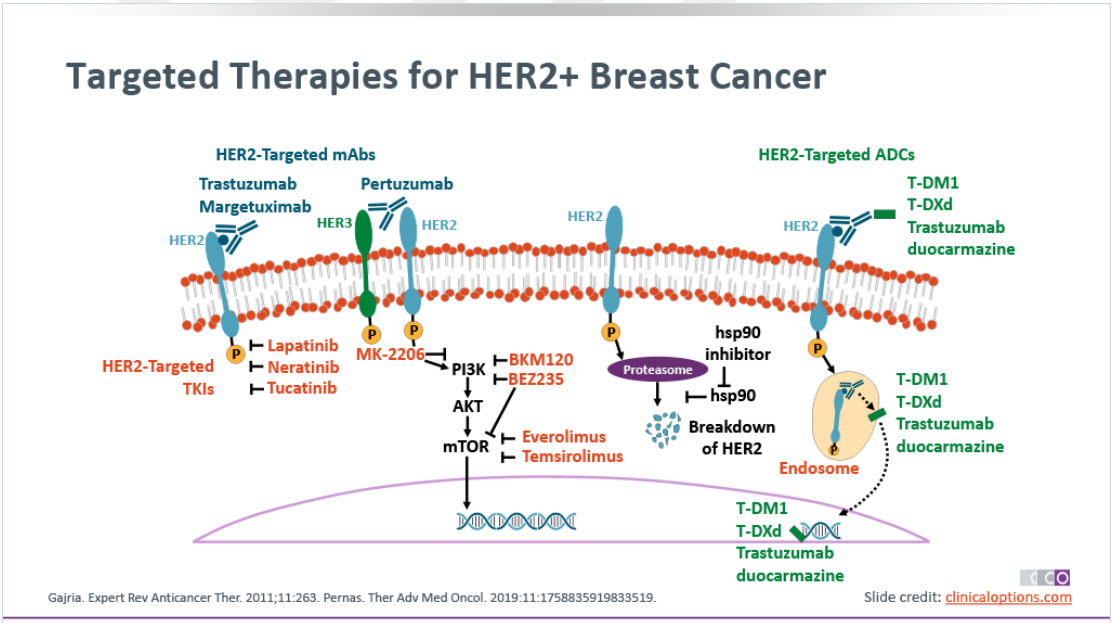


Figure 4.2.1. HER2 targeted therapy

4.2.1. Trastuzumab

Trastuzumab is a monoclonal antibody used against HER2 receptor. Trastuzumab complementary determinant region amino acids complement amino acids located in the IVth domain of the HER2 ectodomain, and binds to them. It has a very important place in the treatment of early and metastatic breast cancer. Combinations of

trastuzumab and chemotherapy started to be used approximately 15 years ago. It has been shown to importantly high survival in HER2-positive cancer patients (22,23) Trastuzumab was administered weekly (4 mg / kg intravenous loading dose followed by 2 mg / kg IV weekly) in the first clinical trials. With subsequent studies, it has been shown that it is more appropriate to administer 6 mg / kg (with a loading dose of 8 mg / kg) every three weeks. Recorded data show that trastuzumab significantly improves the patients' quality of life with the introduction of chemotherapy for HER2-positive breast cancer patients (21,24–26).

Trastuzumab is an IgGl. Two mechanisms of function mediated by Fab or Fc regions are proposed. Fab comprises the antigen binding sites of the antibody while Fc comprises the binding sites for Fc receptors found on immune cells, platelets, hepatocytes, and endothelial cells (27–29).

Besides the fact that trastuzumab provides effective treatment in HER2 positive breast cancer, long-term use of trastuzumab triggers the development of a resistance mechanism. As a result, cancers resistant to trastuzumab occur. Therefore, understanding the trastuzumab resistance mechanism is of great importance. The mechanisms of trastuzumab resistance can be examined under 4 headings. First, the barriers to the binding of trastuzumab to HER2 are the up-regulation of HER2 downstream signaling pathways, signaling via alternative pathways, and finally the inability to trigger immune-mediated mechanisms to destroy tumor cells. These models have been validated preclinically but have not yet been validated in clinical samples (27).

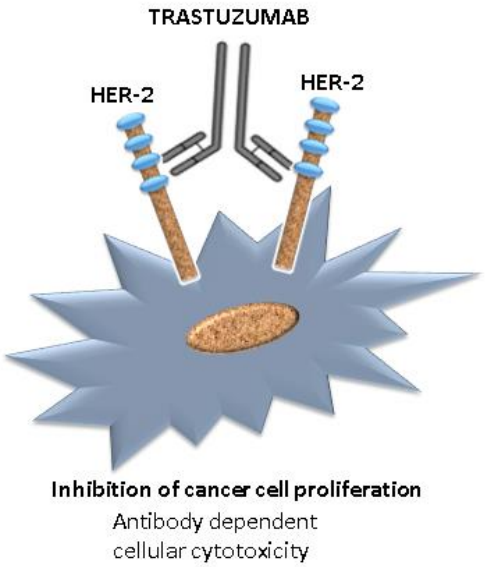


Figure 4.2.1.1. Mechanism of action of Trastuzumab

4.2.2. Pertuzumab

Pertuzumab is a recombinant, humanized monoclonal antibody. Trastuzumab binds to the extracellular dimerization domain IV of HER2, while pertuzumab binds to the extracellular dimerization domain II of HER2. In addition, while trastuzumab inhibits HER2 dimerization by binding close to the transmembrane domain, pertuzumab inhibits HER2 heterodimerization with other HER family receptors by binding to the dimerization domain(30). It can also inhibit tumor cell growth following HRG-induced HER2 heterodimerization(31). Both antibodies cause antibody-dependent cell-mediated cytotoxicity. In this way, inhibition of the activation of downstream cell signaling pathways critical for tumor growth occurs (32–35).

As mentioned earlier, trastuzumab and pertuzumab have different ways of working, and these pathways are likely to complement each other. The combination of both antibodies provides a strong blockade of HER2 downstream signaling (Figure 2). According to a clinical trial, the combination of pertuzumab, trastuzumab, and docetaxelle in patients with HER2-positive metastatic breast cancer was noted to significantly prolong both progression-free survival and overall survival (36,37).

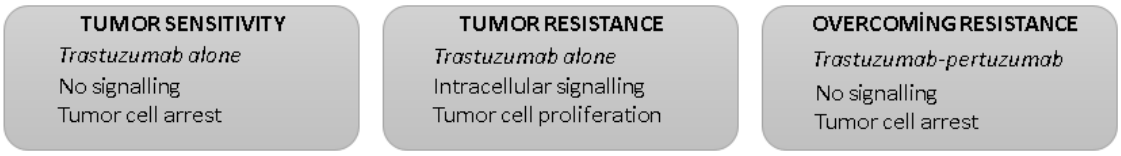


Figure 4.2.2.1. Mechanisms of pertuzumab and trastuzumab

4.2.3. Ado Trastuzumab emtasine

Ado-trastuzumab emtansine (also known as T-DM1) is a HER2-targeted antibody-drug construct that is bound to trastuzumab with the antimicrobial agent emtansine. T-DM1 provides intracellular delivery of DM1 (maytansine derivative) to HER2-overexpressing cells and maintains trastuzumab activity in this process(38). This drug-antibody conjugate is approved for HER2-enhanced or overexpressing metastatic breast cancer patients are available(39).

4.2.4. Lapatinib

Lapatinib is a small molecule that inhibits both HER2 and EGFR kinases. Studies have shown that lapatinib treatment in MCF-7 cell line reduces downstream phosphorylation of AKT and MAPK pathways and inhibits cell growth. It has also been noted to inhibit the growth of tumors in xenograft models (40). In a phase III study, the addition of lapatinib resulted in an improvement in time to progression compared to chemotherapy alone, resulting in FDA approval for the treatment of advanced or metastatic patients(41). In another study, lapatinib Pyruvate kinase inhibits cell proliferation in breast cancer by affecting muscle isozyme (PKM2) expression (42).

4.3.Information on Glycolysis

Glycolysis occurs in the cytoplasm. It converts glucose into pyruvate, lactate and hydrogen ions. As shown in figure-4.3.1 in the first step, glucose transport is an important factor in aerobic glycolysis to protect tumor cells from high glucose consumption. The glucose transporters Glut-1 and sodium-glucose-dependent

transporter 1 (SGLT1) have been found to be overexpressed in most cancer cells (43,44). In the first step, intracellular glucose is phosphorylated to glucose-6-phosphate by the HK-2 enzyme. This product is converted to fructose-6-phosphate with the help of glucose-6-phosphate isomerase enzyme. Downstream of PGI modulates degradation of F-1,6-P to G6P via G6P to 6-phosphofructokinase (PFK) and fructose1,6-biphosphatase (FBPase) activities(45). During the glycolytic pathway, F-1,6-P is converted to glyceraldehyde-3-phosphate by the enzyme aldolase (ALDO). Among the three ALDO isoforms, ALDO B is overexpressed in cancer cells (46). In addition to ALDO, glyceraldehyde 3-phosphate can be rapidly produced from dihydroxyacetone phosphate by triosephosphate isomerase (TPI). High regulation of TPI has been reported in many cancer types. In the next step, glyceraldehyde 3-phosphate is dehydrogenated. Glyceraldehyde is converted to 1,3-bisphosphoglycerate by the enzyme phosphate dehydrogenase (GAPDH). After 1,3-bisphosphoglycerate production by GAPDH, a 1,3-bisphosphoglycerate phosphate group is transferred to ADP by phosphoglycerate kinase (PGK) to form ATP and 3-phosphoglycerate (47,48). 3-phosphoglycerate is then converted to 2-phosphoglycerate with the help of the enzyme phosphoglycerate mutase (PGM). It is then converted to phosphoenolpyruvate by 2-phosphoglycerate enolase (ENO) (49,50). All of the above mentioned enzymes are known to be overexpressed in various cancers(51–53)

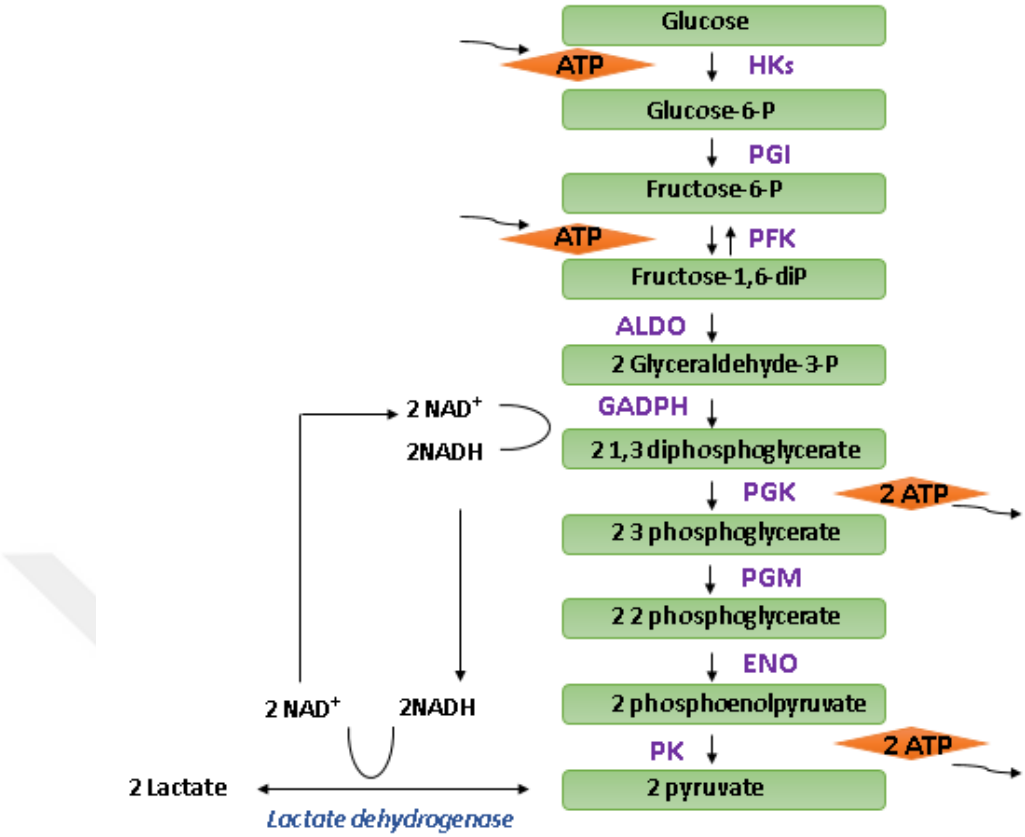


Figure 4.3.1. Biochemical Transformation of Glucose

4.4.Glycolyse in Cancer Cells; Warburg Effect

Inhibition of glycolysis in cancer cells is associated with mitochondrial respiratory dysfunction and hypoxia. It also offers a strategy for overcoming drug resistance(54). The development of safe and effective new therapeutic strategies depends on a better understanding of the difference between cancer cells and normal cells. One of the main biochemical features in most cancer cells is that they produce energy by increasing the rate of aerobic glycolysis. In addition, cancer cells prefer glycolysis instead of oxidative phosphorylation. Therefore, changing the shape of energy metabolism, which is a biochemical fingerprint of cancer cells, has been accepted as one of the 'characteristics of cancer. A series of cancer cell behaviors such as endless proliferation and metastasis consumes a large amount of energy. To get used to this state, cancer cells need to raise their glucose as glycolysis is less efficient than oxidative

phosphorylation on adenosine triphosphate (ATP) yield. Therefore, targeting glycolysis is a promising strategy for metastatic cancer. According to new research, inhibition of glycolysis kills cancer cells. It also shows that it has a mild effect on normal cells. A single drug that inhibits glycolysis is widely used in chemotherapy (55).

The Warburg effect is associated with increased glycolysis. Therefore, there is an increase in the HK2 level. The increase of HK2 has an important place in tumor development and progression. In this context, its first step in glycolysis is the enzyme hexokinase, which controls the phosphorylation of glucose to form glucose-6-phosphate (G6P). HK2 is an important enzyme that controls the first step of glycolysis. There are studies showing that inhibition of HK2 inhibits cancer cell proliferation without overt side effects in animal models (56), suggesting that targeting HK2 is a viable strategy for cancer therapy (56). The increase in HK2 enzyme level is an important difference between cancer cells and normal cells. This may lead to the development of new strategies to target and kill cancer cells(57). Mito-HKII plays a cytoprotective role by protecting the mitochondrial membrane integrity and supports the metabolic coupling of glycolysis and oxidative phosphorylation(58). Thus, HK2 inhibition causes a significant reduction in glycolysis, which affects multiple pathways of central metabolism and also stabilizes the mitochondrial outer membrane, ultimately increasing cell death(56).

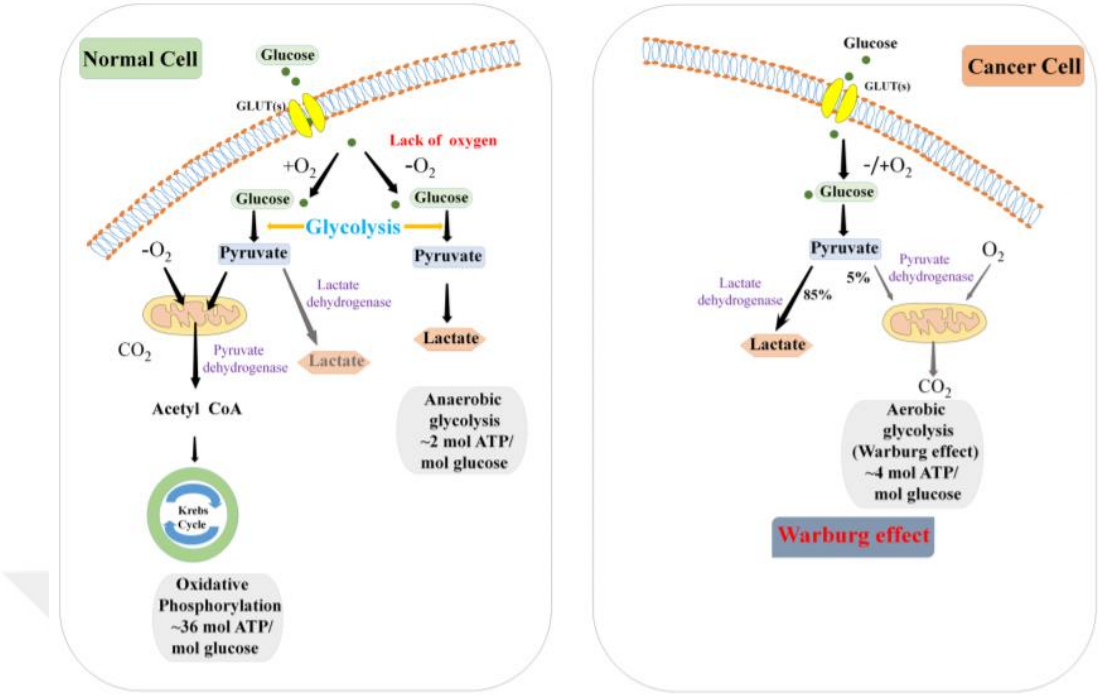


Figure 4.4.1. Differences between oxidative phosphorylation, anaerobic glycolysis and aerobic glycolysis(59)

4.5.Hexokinase 2 (HK2)

Hexokinase 2 is an enzyme that in humans is encoded by the HK2 gene on chromosome 2. This gene encodes the enzyme hexokinase 2, the predominant form found in skeletal muscle. It is localized in the outer membrane of mitochondria48. Hexokinase (HK) converts glucose to glucose-6-phosphate (G-6-P). This G-6-P then initiates important glucose pathways including glycolysis, the pentose phosphate pathway. HK is an indispensable regulator of glucose metabolism (60). In addition, it has been reported that increased hexokinase concentrations together with decreased glucose-6-phosphatase ratios accelerate glucose phosphorylation, resulting in increased glucose consumption(61).Therefore, the HK family of enzymes functions to catalyze the first irreversible step of glycolysis, in which glucose is phosphorylated to glucose-6-phosphate(62). Although HK isoforms are differentially expressed in various tissues, hexokinase 2 (HK2) is considered one of the most important subtypes for glucose metabolism in cancer cells(63).

Expression of the HK2 gene is insulin sensitive. According to studies in rats, it has been shown to play a role in increasing glycolysis in rapidly proliferating cancer cells(64,65). In addition, the mechanism of increased glycolysis in cancer cells has been described as the Warburg effect.

4.5.1. HK2 Inhibitors

HK2 is a new tumor inhibitory target. However, several potent HK2 inhibitors have been identified. Currently, 2-Deoxyglucose (2-DG) and 3-Bromopyruvate (3-BrPA), lonidamine are the most reported HK2 inhibitors. 2-DG works as an HK2 inhibitor by replacing glucose. Since the 2-hydroxyl group is replaced with hydrogen, it cannot enter glycolysis anymore, thus stopping the glycolysis step(55,65). As it can be understood from here, it is not a complete HK-2 inhibitor and as a single agent, it does not have a important therapeutic activity due to the dose range of 500-2000 mg / Kg in mice. As for 3-bromopyruvic acid (3-BrPA), halogenated pyruvate, and strong alkylating agent, of cysteine residues towards free SH groups in proteins, it has no use because it can affect multiple enzymes and cause inevitable side effects, is unstable, and only shows inhibition of glycolysis at high concentrations. Another drug is lonidamine (also called TH-070)(66,67). Lonidamine, which inhibits energy metabolism in cancer cells and increases the activity of other anti-cancer agents, has been clinically studied in different cancer types such as benign prostatic hyperplasia, glioblastoma multiforme, ovarian cancer, and lung cancer, and has taken its place among supportive anti-cancer agents (44,68). However, its use has been suspended due to toxicity problems. It seems possible to inhibit the increased glycolysis that occurs in cancer cells with the least toxicity, by developing the mechanism that lonidamine can have a high effect at low doses(69).

4.5.2. The Relationship of HK2 and Apoptosis

When we look at the relationship of apoptosis mechanism with HK2 inhibitors, it is seen that it is at the center of the event and is at the key point for the occurrence of apoptosis(70). HK2 mediates the ATP-mediated conversion, phosphorylation, of glucose (or other hexose sugars) to glucose-6-phosphate depending on ATP. It does

this depending on the mitochondria. Mitochondrial binding helps increase selectivity as it is a property of hexokinase I and II isoforms only. HK2 binds to the mitochondrial outer membrane with high affinity. This binding is associated with the interaction with the voltage-dependent anion channel(VDAC)(71,72). According to this, binding of HK2 to the mitochondrial membrane occurs through interaction with the outer membrane protein VDAC, which activates the apoptotic process. Thus, HK2 binding to VDAC can suppress the release of its proteins into the intermembrane space and inhibit apoptosis. Thus, it may contribute to tumor cell survival (73). When we examine this mechanism in detail, Akt can directly phosphorylate HK2. AKT also negatively regulates glycogen synthase kinase 3β (GSK3β) activity and VDAC phosphorylation. In this way, HK2 binding to mitochondria is affected. GSK3β can phosphorylate VDAC-1 on threonine 51, which allows HK2 to dissociate from VDAC-1 and affect cancer cells by chemotherapeutic agents (74). Dissociation of HK-2 from VDAC results in disruption of the BCL-XL-BAX interaction and binding of BCL-XL to VDAC. The BCL-XL version facilitates BAX binding, which prevents BAX-BAK interaction and guards against OMM pass-through. The formation of pore structures that allow the released BAX to communicate with BAK and the release of cytochrome-c and other apoptosis proteins in the outer membrane is ensured. This leads to the initiation of apoptosis (75).

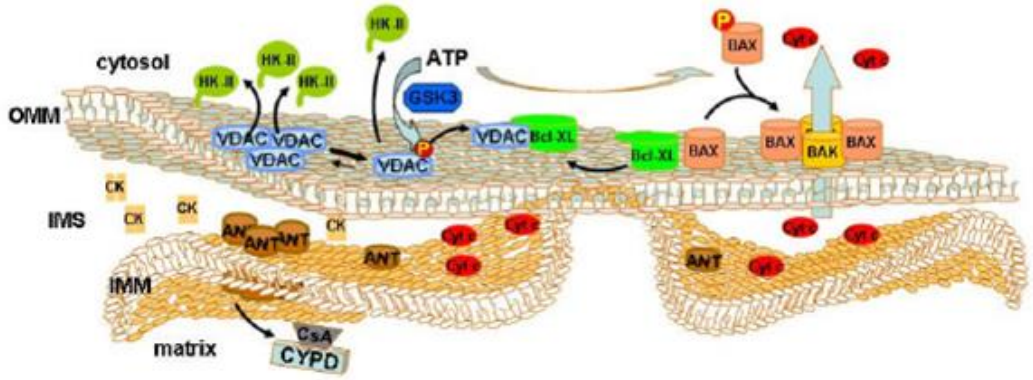


Figure 4.5.2.1. Dissociation of HK2 and its effect on apoptosis(74)

4.5.3. The Relationship of Tmab and HK2

Tumor therapy zresponse estimation can be determined by positron emission tomography (PET) to monitor changes during therapy. 2-[18F]-Fluoro-2-deoxy-D-glucose (FDG) is the most widely used PET tracer available at all PET centers. There are many studies showing that continuous FDG-PET research in cancer patients during chemotherapy is an important method in cancer management (76). Generally speaking, FDG uptake is reduced within a few days of starting chemotherapy when responsive tumors are compared with pretreatment. Two studies of human tumor xenografts have produced conflicting results regarding the effect of trastuzumab response on FDG participation. McLarty et al. It was shown that treatment of HER-2 highly expressing MDA-MB-361 cells showed a decrease in FDG, whereas MDA-MB-231 cells that did not overexpress HER-2 showed no change in FDG regulation (77). However, Shah et al found that FDG incorporation by trastuzumab-treated MMTV/HER-2 and BT474 cells was not accompanied by response (78). As a result of these studies, some studies have revealed that inhibiting HER2 with Tmab also affects HK2. In these studies, Chenye RW et al. In his first study, Tmab not only inhibited HER2, but also stated that this inhibition decreased the expression of HK2 and accordingly FDG combination decreased (79). Later, Smith TA et al. demonstrated this effect with their xenograft model with mice (80). Cooper et al. reported that the co-administration of Trastuzumab and Metformin increased the fraction of phosphorylated [18F]FDG in cells compared to control cells, in a relationship demonstrated by previous studies, and that HK2 efficiency increased with MET (80–82). KU004, a new quinazoline derivative molecule, with structural modification based on lapatinib, studies have been done that it is a HER2 inhibitor. He later stated that this molecule was both an HER2 and HK2 inhibitor. However, as mentioned above, HER2 inhibition also reduces HK2 expression (82,83).Therefore, although the drug found is not an HK2 inhibitor; It has been shown that the effects of HER2 and HK2 are parallel and that inhibiting HK2 together with HER2 will have a positive effect on the tumor.

When the relationship between the HER2 receptor and the HK2 enzyme is examined in terms of apoptosis; As mentioned above, AKT is the common point of both. Therefore, both HK2 and HER2 suppress apoptosis and cause uncontrolled

proliferation of cells. Inhibition of HER2 with Tmab prevents suppression of apoptosis and ensures cell death. However, resistance to Tmab prevents long-term use of the drug. It has been shown that activation of the PI3K/AKT signaling pathway can lead to resistance to HER2-positive Tmab in this development of resistance (84). Since AKT activation stimulates aerobic glycolysis in cancers, it is assumed that the Warburg effect may increase and lead to Tmab resistance (85). At the same time, since AKT is involved in many vital pathways, inhibiting HK2 instead of AKT will help to induce apoptosis and increase efficiency without affecting other pathways. Targeting these two pathways together may be successful against cancer by both preventing resistance to Tmab and further inducing apoptosis.

Metformin (MET), a widely used anti-diabetic drug, has recently been the subject of research with its anti-tumor effect. In this context, in studies where Tmab and MET were given together, it was observed that when used as a neoadjuvant, it reduced the resistance and increased the success rate. Considering the mechanistic descriptions of this effect, it is thought that MET inhibits the erbB2/IGF-1 receptor (86,87). However, recent studies on the anti-cancer mechanism of MET present evidence that it may be an HK2 inhibitor (88,89). It is known that MET has anti-cancer properties by inhibiting HK-2 in studies performed independently of Tmab.

Therefore, it is important to prevent the development of resistance and metastasis, which are among the problems encountered in the treatment of HER2 positive breast cancer patients. Also suggests that this situation may open the door to new ideas that will increase the drug efficacy by stopping the energy pathways of cancerous cells and triggering apoptosis.

4.6.Drug Delivery Systems

Drug development systems refer to the approaches, manufacturing techniques, formulations, storage systems, and technologies involved in drug delivery, delivery of a pharmaceutical compound to the target to achieve the desired therapeutic effect(90,91). Drug development systems target targeted specific therapy by loading drugs into nanoparticles. Nanomedicine is a new and rapidly evolving field(92). Nanotechnology offers numerous benefits in the treatment of chronic human diseases

through the delivery of site-specific and targeted precision drugs. Targeted therapy with nanoparticles ensures that the drug only acts on the target area. The dose of the drug used in this way can be reduced. In addition, toxicity that may occur in healthy cells can be prevented. Drug delivery systems, besides drug loading, can be actively delivered by the addition of targeted ligands such as mAb, antibody fragments, small peptides, vectors, or avidin-biotin complexes(93–95)

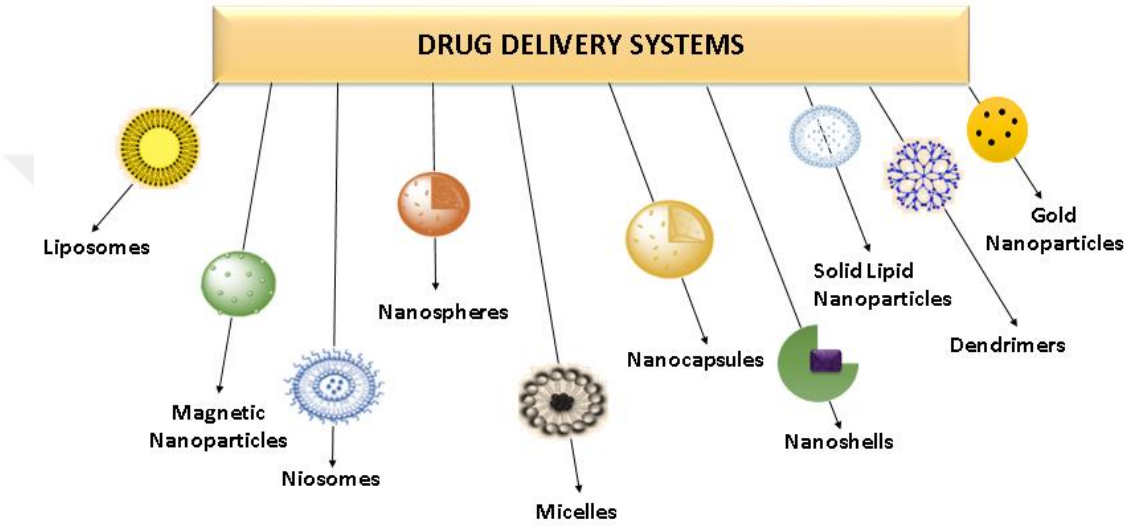


Figure 4.6.1. Drug delivey systems

5. MATERIALS AND METHODS

5.1. Materials

The consumables used in our study are shown in the table below, along with their brand.

Consumables	Company name
Femto-ECL	Thermo
APS	Sigma
TEMED	Biofroxx
Trizmabase	Sigma
HCl	Merck
NaOH	Merck
2X Laemmli Loading Buffer	Sigma
Protein marker	BIO-RAD
Glycin	Sigma
NaCl	Sigma
MetOH	Merck
SDS	Sigma
RIPA	Thermo
Proteaz/Fosfataz ınhibitors	Roche
Pipette tips	Gilson
15 ml falcon	Nest
50 ml falcon	Nest
PVDF membran	GVS
FilterPaper	BIO-RAD
Tween20	Sigma
Acrylamide/BisAcrylamide	Ambion
PBS	PanBiotech

beta mercaptoethanol	BIO-RAD
BSA	Bioshop
Anti-B-actin Rabbit	Abcam
Anti-Rabbit	Abcam
Anti-HER2 Rabbit	Abcam
Anti-HK2 Rabbit	Abcam
Anti-VDAC Rabbit	Abcam
Anti-PARP Rabbit	Abcam

5.2. Devices

Devices used in the studies: Refrigerated Centrifuge (ThermoScientific, USA); Water Bath (Nüve, Turkey); Nanophotometer (Implen, Germany); Western Blot Tank (Invitrogen, USA); Power Supply (Biorad, USA); Transblot Turbo Transfer System (Biorad, USA); Membrane Imaging Device (BioRad, USA); Vortex (Stuart, UK); Pure Water Device (ELGA, UK); Ultrapure Water Device (ELGA, UK); Freezer (-20°C, Siemens, Germany); Freezer (-80°C, Aucma, China); Heated block (Techne, UK); Shaker (Stuart, UK).

5.3. Buffer Solutions

The consumables used in the thesis are shown in the table below.

Table 5.3.1. Blocking Buffer

Blocking Buffer (100 ml)	
BSA	5 gr
TBST	It is completed to 100 ml.

Table 5.3.2. Running Buffer

Running Buffer 10X (1000 ml)	
Trizma base	30.3 gr
Glisin	144 gr
SDS	10 gr
dH_2O	It is completed to 1 lt.

Table 5.1.3. Transfer Buffer(10X)

Transfer Buffer 10X (1000 ml)	
Trizma base	30.3 gr
Glisin	144 gr
dH_2O	It is completed to 1 lt.

Table 5.3.2. Transfer Buffer(1X)

Transfer Buffer 1X (1000 ml)	
Transfer tamponu (10X)	It is completed to 100 ml.
Metanol	200 ml
dH_2O	700 ml

Table 3.3.5.TBST Preparation

TBST 10X (1000 ml)	
Trizma base	24 gr
NaCl	88 gr
Tween 20	10 ml
HCl	PH 7.6
dH_2O	It is completed to 1 lt.

Table 4.Stripping Buffer

Stripping Buffer (1000 ml)	
Glisin	0.2 M
Tween 20	%0.1
HCl	PH 2.5

5.4.Cell Culture Studies

The human HER2 positive breast cancer cell line was incubated at 37 °C, 5% CO2, and 95% relative humidity by adding 10% (v/v) fetal bovine serum (Gibco BRL) to a mixture of high glucose dmem and medium. During the passage, cells were washed with phosphate buffer (PBS) and incubated briefly with 0.25% (w/v) trypsin / 0.53 mM EDTA (Gibco BRL) to separate them in the cell culture dish. Centrifugation was performed at 1200 rpm for 5 minutes to ensure that the separated cells were removed from the trypsin. Media was added to the pellet and pipetted to suspend the cells. Cells were diluted 1:5 and transferred to a T75 cell dish and passaged every 3 days.

5.5. Preparation of Liposome Based Hybrid Nanoparticle Formulations

Nanoprecipitation technique was used to prepare lonidamine-loaded liposome-based hybrid nanoparticles. A series of formulations were prepared using lonidamine added at 5%, 10% and 20% (w/w) ratios of the selected PLGA polymer to form the polymeric core of the hybrid structure. Stock solutions were prepared by dissolving lonidamine and PLGA polymer in acetonitrile, and DSPE-PEG-COOH and phosphatidylcholine were separately dissolved in a 4% ethanol-water mixture to form the liposome-based shell structure of the hybrid system. Calculated amounts of DSPE-PEG-COOH 2000 and phosphatidylcholine stock solutions were added to distilled water within the ratios presented in Table 1 and sonicated in an ultrasonic bath at 35°C at 40 kHz ultrasonic power. The nanoparticle dispersion was centrifuged at 4500 rpm using Vivaspin 20 (Sartorius) centrifuge filters in order to remove the free excipients and uncharged active substance in the environment. The obtained liposome base hybrid nanoparticle

concentrate was frozen for 1 day at -80°C and then lyophilized for 2 days (Christ gamma 2-16 LSC, Martin Christ Gef., Germany) and stored at 4°C until use(96). Empty nanoparticles that do not contain lonidamine were produced in the same way, only the active substance was not added to the formulations. Formulations containing lonidamine were coded with the code DF, while the blank formulation without lonidamine was coded with the code BF.

Table 5.5.1. Contents of lonidamine-loaded liposome-based hybrid nanoparticles

Formula Code	Formulation Ingredients						
	Organic phase			Water phase			
	PLGA (µg)	Lonidamine (µg)	Asetonitrile (µl)	DSPE-PEG-COOH 2000 (µg)	Phosphothi-dylcholine (µg)	%4'lük Ethanol (µl)	Distille * water (ml)
DF1	4000	200	1600	800	50	850	ym 16
DF2	4000	400	1600	800	50	850	ym 16
DF3	4000	800	1600	800	50	850	ym 16
BF	4000	-	1600	800	50	850	ym 16

5.6.Characterization of Liposome Based Hybrid Nanoparticle Formulations

5.6.1. Determination of Encapsulation Efficiency

In order to determine the amount of lonidamine contained in the nanoparticles, 2.5 mg of lyophilized nanoparticle in acetonitrile was sonicated in an ultrasonic homogenizer for 10 minutes, and the amount of active substance contained in the nanoparticles was determined by reading the absorbance at 298 nm wavelength in the UV spectrophotometer (n=3). The encapsulation efficiency (%) values of nanoparticles were calculated using the equations given below(97).

$$\% \text{ Active Ingredient Loading Capacity} = \frac{\text{The amount of active substance in the nanoparticle}}{\text{Nanoparticle amount}} \times 100$$

$$\% \text{ Theoretical Active Ingredient Amount} = \frac{\text{The amount of active substance in the disperse phase}}{\text{The amount of solids in the disperse phase}} \times 100$$

$$\% \text{ Transaction Activity} = \frac{\% \text{ Active ingredient loading capacity}}{\% \text{ Theoretical amount of active substance}} \times 100$$

5.6.2. Determination of Particle Size, Size Distribution (PDI) and Surface Charge

Photon correlation spectroscopy Zetasizer Nano ZS instrument was used to determine polydispersity index (PDI), particle sizes and zeta potential values of liposome-based nanoparticle formulations. For this purpose, analyzes were made by placing nanoparticles dispersed in distilled water into the relevant chamber of the device (n=3).

5.6.3. Determination of Morphological Characteristics

Transmissive Electron Microscopy (TEM) analysis was used to visualize the shapes of the liposome-based hybrid formulations. For imaging purposes, hybrid nanoparticles in the form of aqueous dispersion were dropped onto the carbon film covered with copper sheet and left overnight in a petri dish with a lid and dried at room temperature. Samples prepared in this way were stained with 2% (w/v) uranyl acetate solution before being visualized.

5.6.4. Determination of In Vitro Active Substance Release Rate

Dialysis membrane technique, which is a static method, was applied to determine the release rate and release profile of lonidamine from liposome-based hybrid nanoparticle formulations. For this purpose, nanoparticles suspended in dialysis membranes with a molecular size of 12-14 kDa at appropriate rates were placed in 75 ml of PBS pH 7.4 phosphate buffer at 37°C. The prepared systems were incubated in a shaker with an incubator at a rotational speed of 75 rpm (n=3) and 1.5 ml of sample was taken at

predetermined time intervals and the amount of lonidamine released was analyzed in a UV spectrophotometer at a wavelength of 299 nm.

5.7. Cell Viability Analysis

The SKBR3 (HER2 positive breast cancer) cell line was cultured in a 37°C incubator with 5% CO_2 in high glucose medium containing 10% FBS. When the cells covered 80% of the culture surface, after washing with PBS, they were removed using 0.25% Trypsin-EDTA (Gibco) and cells were seeded into 96-well black plates (Corning) ($1x10^4$ cells/well). After 24 hours of incubation, the drug was given to the cells, which had reached sufficient density, in triplicate wells for each dose. It is planned to use a total of seven control groups, including untreated cells, as controls. LND will be used as HK2 inhibitor. In the literature, LND studies are performed at 48 or 72 hours, while in Tmab studies, the effective dose is given at 72 or 120 hours. Cell viability testing was performed using the CellTiter-Glo® Luminescent Cell Viability Assay protocol.

5.8. Annexin V Apoptosis Assay

Detection of apoptosis was performed using the eBioscience™ Annexin V Apoptosis Detection Kit FITC. The experimental steps were followed as follows.
Firstly, wash the cells in PBS(1X) by shaking or pipetting. Centrifuge and obtain a cell pellet. Resuspend cells in Binding Buffer(1X - 200 µl), cell density should be $2\text{-}5.10^5$. Then, centrifuge and obtain a cell pellet. Add 5 µl(1-5) Annexin V-FITC to 195 µl cell suspension. Mix and incubate for 10 minutes at room temperature. Centrifuge and obtain a cell pellet. Wash cells in Binding Buffer(1X - 200 µl) and resuspend in Binding Buffer(1X - 190 µl). Add 10 µl Propidium Iodine (20 µg/ml). Lastly, perform FACS analysis.

5.9.Apoptotic DNA Ladder Kit

A sample volume of $2x10^6$ cells is used. 200 µl of Binding/Lysis Buffer is added to a final volume of 400 µl. It is then mixed immediately. Incubate for 10 minutes at +15 to +25 ºC. 100 µl of isopropanol is added to the samples and positive control after 10

minutes of incubation. It should then be shaken. A filter tube and a collection tube are combined. The sample is pipetted into the upper chamber. Centrifuge for 1 minute at 8,000 rpm in a standard benchtop centrifuge. The flowthrough is discarded. The filter tube and the used collection tube are reassembled. Add 500 µl of Wash Buffer to the upper chamber. Centrifuge for 1 minute at 8000 rpm. The flow is discarded and the filter tube and used collection tube are recombined. Add 500 µl of Wash Buffer to the upper chamber. Centrifugation is performed at 8000 rpm for 1 minute. Finally max. It is centrifuged for 10 seconds. The speed should be 13,000 rpm to remove any remaining Wash buffer. Discard the collection tube and place the filter tube in a clean 1.5 ml tube. Elution of DNA: 200 µl of pre-warmed (+70 ºC) Elution Buffer is used. A higher elution volume can also be used to increase elution efficiency. Add Elution Buffer to the filter tube. Centrifugation is performed at 8000 rpm for 1 minute.
DNA is obtained stably. It can be used directly or stored at -15 to -25 ºC (do not store more than 14 days).

5.10. PCR and Real Time PCR

Optimization was made to determine the appropriate temperature for the primers before real-time PCR was performed.

5.10.1. Total RNA isolation from cell

Total RNA isolation was performed using the GeneJET RNA Purification Kit (Thermo Scientific, USA). The isolation process steps are shown in order;
1. Cell blasting solution (lysis) was prepared by adding 20 µl of 14.2 M β-mercaptoethanol into 1 ml of Lysis buffer. By using 600 µl of this solution, the pellets were suspended by pipetting.
2. 360 µl of 96% ethanol was added and pipetting slowly.
3. The entire solution was transferred to the GeneJET RNA collection tube and centrifuged for 1 minute at 15 000 x g at room temperature.
4. After the liquid passed into the collection tube after centrifugation, 700 µl of ethanol-containing washing solution 1 was added and centrifuged at 15 000 x g for 1

minute.

5. After the liquid passed into the collection tube after centrifugation, 600 µl of ethanol-containing washing solution 2 was added and centrifuged at 15 000 x g for 1 minute.

6. After the liquid passed into the collection tube after centrifugation, 250 µl of washing solution 2 containing more ethanol was added and centrifuged at 15 000 x g for 1 minute.

7. After centrifugation, the collection tube was discarded and the filter tube containing RNA was placed in a new 1.5 ml eppendorf tube.

8. The RNA in the filter tube was drained in 100 µl of nuclease-free water by centrifugation at 15 000 x g for 2 minutes.

9. In order to measure the purity and quality of the obtained RNA samples, the absorbance values at 260/280 nm wavelength were measured by using a spectrophotometer (Thermo Sci. Multiskan go, Finland) device.

10. Finally, the quality of the RNA bands was ensured in 1% agarose gel electrophoresis. To prepare agarose gel electrophoresis, 1 g of agarose was dissolved in 100 ml of TAE buffer. Then, 5 µl of Redsafe gel dye was added into it and waited for it to freeze. RNA bands were visualized using gel imaging system.

5.10.2. DNase treatment

After RNA isolation, RNAs were treated with DNase and thus DNA contaminant was removed. For this, DNase 1 (Thermo scientific, USA) kit was used. The solution and amounts used are shown in Table 5.9.2.1. The amounts to be used for DNase were calculated according to the concentrations of the RNA samples. After adding 10X $MgCl_2$ buffer solution, RNA and DNase 1 enzyme, the final volume of the reaction was completed to 10 µl and incubated at 37˚C for 30 minutes in a thermalcycler (Thermo). After the incubation was completed, 1 µl of 50 mM EDTA was added to the reaction tubes and incubated at 65 minutes for 10 minutes in the thermalcycler.

Table 5.9.2.1.DNase reaction components and quantities

DNase Reaction Components	Quantity
RNA	1µg
Reaction buffer containing 10x $MgCl_2$	1µl
Dnaz I	1µl (1U)
Nuclease-free water	The final volume was made up to 10 µl.
50 mM EDTA	1µl

5.10.3. Complementary DNA synthesis

The RNA samples cleared after DNase treatment were converted into complementary DNA with the help of the reverse transcriptase enzyme included in the kit, using the iScript cDNA synthesis kit (BIO-RAD, USA). Reaction amounts are shown in Table 5.9.3.1.

Tablo 5.9.3.1. Complementary DNA synthesis components

Complementary DNA synthesis components	Quantity
5x iScript Reaction Mix	4 µl
iScript Ters Transkriptaz Enzimi	1 µl
RNA	2 µg
Nuclease-free water	The reaction was completed to the final volume of 20 µl.

The reaction was completed to 20 µl with water after adding 5x iScript Reaction Mix, RNA, iScript Reverse Transcriptase enzyme, respectively. Then, the reaction was incubated at 25 °C for 5 minutes, at 46°C for 20 minutes, and at 95oC for 1 minute in a thermalcycler, and cDNA was obtained. DNA samples were stored at -20 °C until use.

5.10.4. Polymerase chain (PCR) reaction

In order to determine the most suitable binding temperature for primer pairs used in gene expression analyzes of apoptotic, autophagic, and telomerase (Bax, Bcl-2, MPP-2, GAPDH) activity, classical PCR was performed by temperature gradient method using cDNAs for each primer pair. The components used in PCR and their amounts are given in Table 3.4. PCR reaction conditions and temperatures are given in Table 9. The PCR reaction was carried out in a thermal cycler, and then the PCR products were carried out in 1% agarose gel electrophoresis at 110 Volts for 45 minutes and the bands were visualized on the gel imaging device. Appropriate band-forming products after PCR reaction were used in the next analysis, real-time PCR reaction, to determine gene expression analyses. The optimized binding temperatures for primer pairs are shown in Table 5.5.4.1.

Table 5.5.4.1.PCR reaction conditions and temperatures

Reaction steps	Temperature	Time	Number of Cycles
Initial Denaturation	95 °C	5 min.	1
Denaturation	95 °C	1 min	35
Primary Binding	53 °C - 62 °C	1 min	
Elongation	72 °C	1 min.	
Final Elongation	72 °C	7 min.	1

Table 5.9.4.2. Components and quantities required for PCR reaction

Necessary ingredients for the reaction	Quantity required for 1 PCR tube
10X tag buffer	2 µl
dNTP mix	2 µl
$MgCl_2$	3 µl
Forward primary	1 µl
Reverse primary	1 µl
Tag DNA polymerase	0,5 µl
Template DNA	100 ng
nuclease-free water	Final volume is made up to 20 µl with water.

5.10.5. Real-time PCR analysis

After optimizing the binding temperatures of the template DNAs to the primer pairs with the classical PCR method, real-time PCR was performed for the determination of gene expression analysis.

Table 5.9.5.1. Primers and coupling temperatures used for the PCR reaction

Primary name	Primary Direction	Primer Sequence (5'→3')	Primer Length	GC rate %	Optimized bonding temperature
BAX	Forward	CCCGAGAGGTCTTTTTCCGAG	21 bp	60	57 °C
	Reverse	CCAGCCCATGATGGTTCTGAT	21 bp	52	
BCL-2	Forward	GGATAACGGAGGCTGGGATG	20 bp	52	57 °C
	Reverse	TGACTTCACTTGTGGCCCAG	20 bp	52	
MMP-2	Forward	TCTCCTGACATTGACCTTGGC	21 bp	52	57 °C
	Reverse	CAAGGTGCTGGCTGAGTAGATC	22 bp	45	
GAPDH	Forward	GGACTGACCTGCCGTCTGA	19 bp	63	57 °C
	Reverse	TAGCCCAGGATGCCCTTGAG	20 bp	60	

For the real-time PCR reaction, each experimental step was performed in triplicate and also run in three biological replicates. Components and temperature conditions used for the reaction Table 5.9.5.2. and are given in Table 5.9.5.3. For Syber green, reading will be made at a wavelength of 530 nm, and melting curve analysis was performed to see if the amplifying gene region is replicating in the right place. The reaction was carried out by Real-time PCR instrument reading with fluorescent signals at each 0.5°C increment between 65°C and 95°C.

Table 5.9.5.2. Substances and quantities used for simultaneous PCR

Simultaneous PCR reaction components	Quantity
Supermix(syber green)	10 µl
Forward Primary	1 µl
Reverse Primary	1 µl
Template cDNA	100 ng
Nuclease-free water	Final volume is made up to 20 µl with water.

Table 5.9.5.3. Conditions for simultaneous PCR reaction

Program	Temperature	Reading	Number of Cycles	Reaction Time
Initial Denaturation	**95 ˚C**	**-**	**1**	**300 sec**
Denaturation	**95 ˚C**	**-**	**39**	**10 sec**
Merger	**57 ˚C**	**-**		**20 sec**
Elongation	**72 ˚C**	**single**		**10 sec**
1. Melting	**95 ˚C**	**-**	**1**	**5 sec**
2. Melting	**65 ˚C**	**continuous**	**1**	**60 sec**
3. Melting	**97 ˚C**	**continuous**	**1**	**-**
Cooling	**4 ˚C**	**-**	**1**	**10 sec**

A reference gene is needed for comparative gene expression analyzes in simultaneous PCR reactions. Reference gene is genes that have different sequence sequences from the target gene that acts as a control in the reaction. In this study, “human GAPDH” was used as a reference gene. Comparative analyzes of gene expression analyzes were analyzed using the $2^{-2\Delta\Delta CT}$ calculation method and expression levels were calculated. Three biological replicates of each analysis were made, statistical analyzes were performed using a one-way ANOVA test, and the difference was considered significant if the P-value was < 0.0001 and < 0,001.

5.11. Scratch Assay

First, SKBR3 cells are seeded in 6-well plates. The seeding density is adjusted to the appropriate number of cells for the SKBR3 cell line to form a confluent monolayer. The cell monolayer is drawn in a straight line with a sterile 10 µl pipette tip after 24 hours of incubation. The old medium was then replaced with a medium containing the tested compounds. The plates are placed in a phase-contrast, computer-assisted microscope. Plates are placed in an incubator for 48 hours. After completion of the incubation, the plates are placed under the microscope to align the photographed area. Images of the scratch were obtained. Images for each sample at 48 hours were quantitatively analyzed using Image J software.

5.12. Protein Isolation and Western Blot Analysis

Western blot technique was applied by grouping as given in the table 5.11.1.

Table 5.11.1. Experimental groups are planned to be used to determine the efficiency of the carrier system.

Application	Is the included in the carrier system?
Control	No
10 µg/ml Tmab	No
50 µM LND	No
50 µM LND loaded liposome	Yes
50 µM Liposome Blank	Yes
10 µg/ml TR/ 50 µM LND	No
10 µg/ml TR/ 50 µM LND loaded liposome	Yes
10 µg/ml TR/ 50 µM Liposome Blank	Yes

5.11.1 Proteins are lysed with Ripa Buffer.

Table 6. Ripa Buffer Recipe

Ripa Buffer Solutions	µl
Ripa Lysis Buffer	970 µl
Sodium Orthovanadate	10 µl
PMSF	10 µl
Protease inhibitor coctail	10 µl

5.11.2. Preparation of Polyacrylamide Gels

As in the prescriptions given in the tables below, the resolving gel is poured first and approximately 500 µl of isopropanol is added to it. The gel freezes in approximately 15 minutes. After the isopropanol is removed, the stacking gel is poured. It is left to freeze for about 10 minutes. Afterward, the comb attached to the upper gel is carefully removed and the sample loading phase is started.

Table 5.11.2.1. Resolving gel recipe

Resolving Gel Recipe (%10)-10 ml	
%40 Akr-BisAkrilamid	3.3 ml
1 M Tris ph:8.8	3.75 ml
10 % SDS	100 µl
10 % APS	100 µl
Temed	6 µl
dH_2O	2.7 ml

Table 5.11.2.2. Stacking gel recipe

Stacking Gel Recipe-5 ml	
%40 Akr-BisAkrilamid	0.83 ml
1 M Tris ph:6.8	0.63 ml
10 % SDS	50 µl
%10 APS	10 µl
Temed	5 µl
dH_2O	3.4 ml

5.11.3. Loading Samples

1. Samples and loading buffer are mixed so that the final concentration of the loading buffer is 1X (2X laemni; !:1).
2. Electrophoresis buffer is prepared.
3. The gel is placed in the tank with the short glass facing the inside.
4. Electrophoresis buffer is filled into the first chamber and then into the tank and the comb is carefully removed.
5. The wells are washed with buffer using a pipette.
6. The samples are boiled at 90 degrees for 5 minutes and loaded onto the gel.
7. 15-30 ug protein loading is done.

5.11.4. Electrophoresis

8. The samples are run at 90 V until the stacking gel passes the end. Run at 130 V until the dye is transferred from the resolving gel to the buffer.
9. Detection of current is determined by looking for bubbles.
10. If a "smiling effect" occurs in the samples, the voltage should be reduced.

5.11.5. Transfer

11. Electrophoresis buffer is poured, glasses are removed.
12. The stacking gel is discarded with the help of a spatula.
13. Transfer buffer prepared as 1X is placed in a container.
14. The apparatuses to be used are wetted in the buffer.
15. The PVDF membrane is kept in methanol, distilled water, and transfer buffer, respectively (ionic equilibrium is achieved).
16. The transfer process is performed using the Biorad system.

5.11.6. Blocking

17. It is prepared with 5% skim milk powder or BSA TBST and the membrane is blocked for 1 hour (80 rpm).
18. After blocking, washing is done with TBST for 5-15-5-5 minutes, respectively (240 rpm).
19. Primary solutions are prepared in required quantities and poured onto the membrane.
20. Incubate overnight on a shaker in a cold room.
21. After incubation, washing is done with TBST for 5-15-5-5 minutes, respectively (240 rpm).
22. It is incubated for 1.5 hours on the shaker with appropriate secondary antibodies.
23. Afterwards, 5-15-5-5 minutes of washing with TBST is done respectively (240 rpm).

5.11.7. Imaging

24. ECL is applied in a dark environment (Approximately 5-10 minutes).
25. Bio-Rad Chemi-Doc XRS was used as the imaging device.
26. After the image is taken in the Image Lab program, analysis is done.

Hexokinase-2 (CST Rabbit Monoclonal 1:1000), HER2 (CST Rabbit Monoclonal 1:1000), and VDAC (CST Rabbit) Monoclonal 1:1000) expressions were investigated by Western Blotting. Expressions of the above proteins were examined. As the experimental method, the procedures given above were followed.

Statistical methods: Obtained data will be expressed as mean ± SD and statistical analysis will be generated using SPSS version 21. Data will be analyzed using Tukey's post hoc test for one-way analysis of variation (One-way ANOVA) multiple comparison. P values <0.0001, <0,0003, <0.0005, <0,001, <0,005, <0,05 will be considered significant.

6. RESULTS

6.1.Findings for Lipid-Based Nanoparticles

6.1.1. Findings for Determination of Encapsulation Efficiency, Particle Size, PDI and Surface Charge of Lipid-Based Nanoparticles

The data obtained for the encapsulation efficiency, particle size, PDI and zeta potential analyzes of the prepared liposome-based hybrid nanoparticles are presented in Table 6.1.1.1, arranged together with the mean value and standard error values.

Table 6.1.1.1. Physicochemical properties of liposome-based hybrid systems.

Formül Kodu	Encapsulation Efficiency (%)	Average Particle Size (nm)	PDI	Zeta Potential (mV)
DF1	81.47 ± 1.28	160.1 ± 5.71	0.121 ± 0.01	-28.9 ± 1.00
DF2	87.13 ± 1.17	175.7 ± 2.16	0.111 ± 0.03	-30.7 ± 1.05
DF3	93.89 ± 2.05	201.4 ± 5.92	0.144 ± 0.02	-31.7 ± 0.35
BF	-	147.8 ± 4.52	0.091± 0.03	-31.7 ± 0.72

6.1.2. Findings Regarding Morphological Characteristics

The micrographs obtained as a result of the TEM analysis carried out in order to determine the morphology of the lonidamine-loaded liposome-based hybrid nanoparticle formulations are presented in Figure 6.1.2.1.

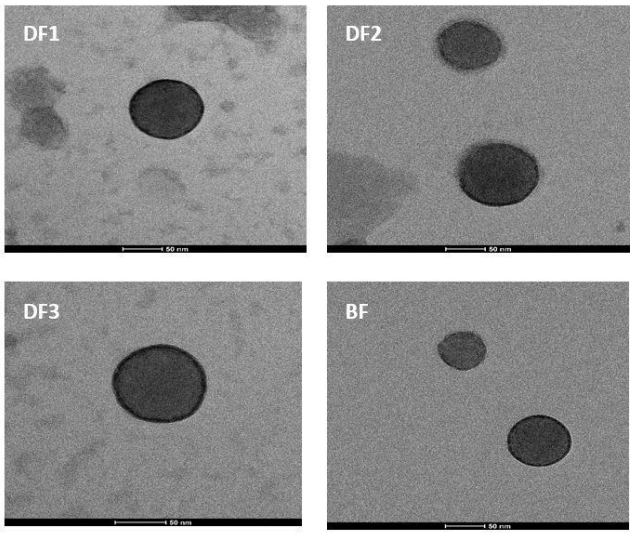


Figure 6.1.2.1. TEM micrographs of lonidamine-loaded liposome-based hybrid nanoparticle formulations.

6.1.3. Findings for the Determination of In Vitro Active Substance Eject Rate

The dissolution rate profiles obtained as a result of the dissolution rate determination for lonidamine-loaded liposome-based hybrid nanoparticle formulations were prepared by plotting the % of active substance released versus time, and presented in Figure 6.1.3.1.

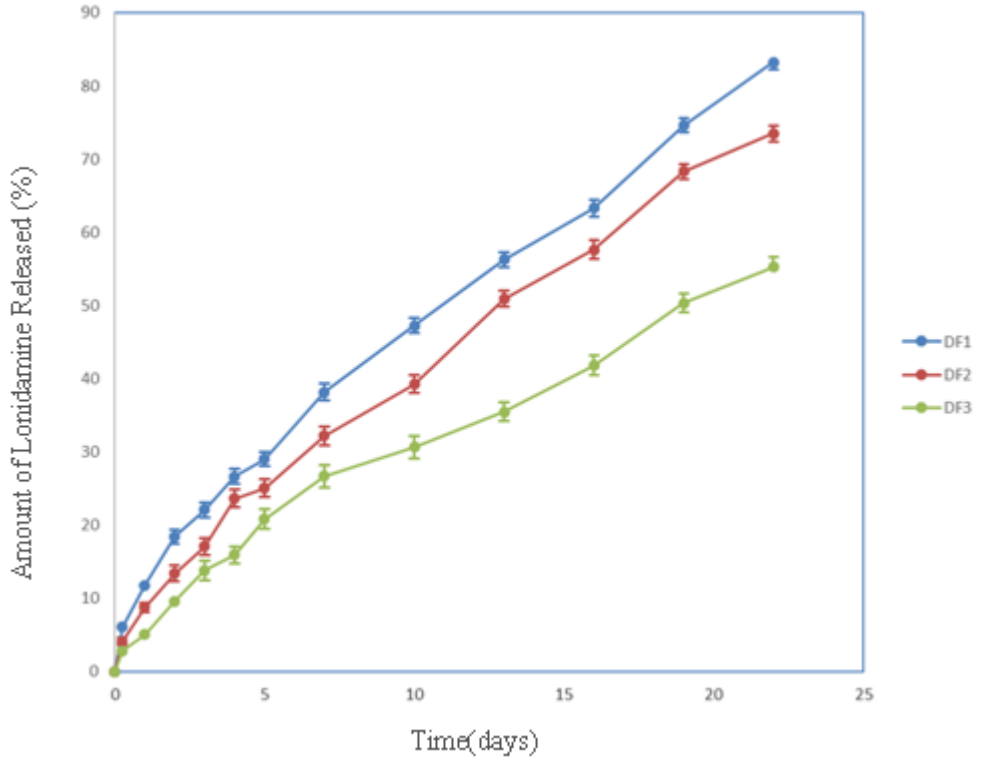


Figure 6.1.3.1. Dissolution rate profiles of lonidamine loaded liposome-based hybrid nanoparticle formulations.

6.2. Cell Viability Analysis

To investigate the effects of Lonidamine, Trastuzumab, Lonidamine-NP, and Blank NP on cell viability in the SKBR3 HER2 positive breast cancer cell line, cells were exposed to the drug. Afterward, cell viability was measured using the CellTiter Glo experiment kit, which is a kit based on the determination of the amount of ATP in the medium.

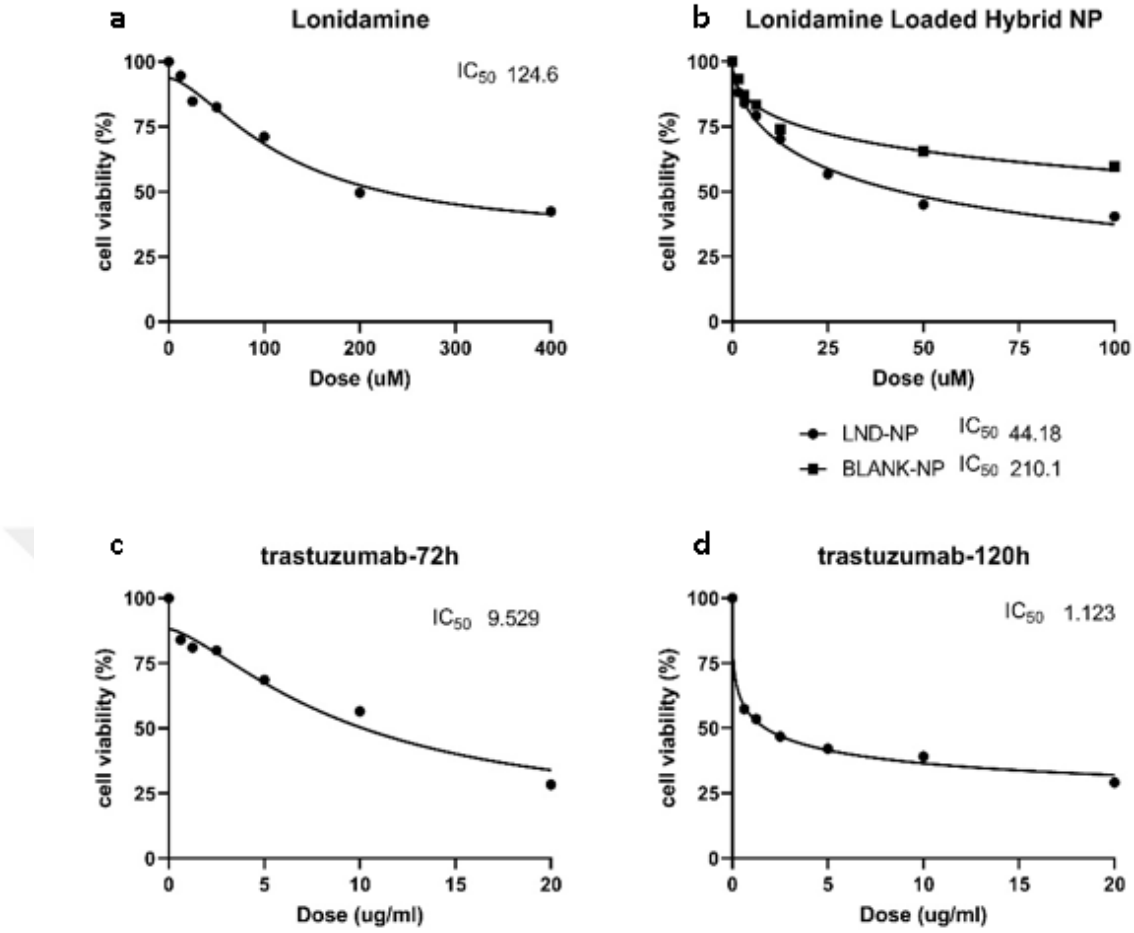


Figure 6.2.1. Determination of IC50 values of drugs and drug delivery system used in the study. a;Lonidamine(48h), b;Lonidamine-NP and Blank-NP(48h), c;trastuzumab(72h), d;trastuzumab(120h)

As seen in the graphs above, Lonidamine, Lonidamine-NP, blank-NP and trastuzumab(72h,120h) gave IC_{50} values of 124.6 µM, 44.18 µM, 210.1 µM, 9.5 µg/ml and 1.12 µg/ml, respectively. Experiments were carried out in 3 repetitions.

6.3. Microscopy Images

Cells were photographed after treatment (48h). Morphological observations were made. Significant morphological changes were observed in the combination groups(Fig 6.2.1 and Fig 6.2.2).

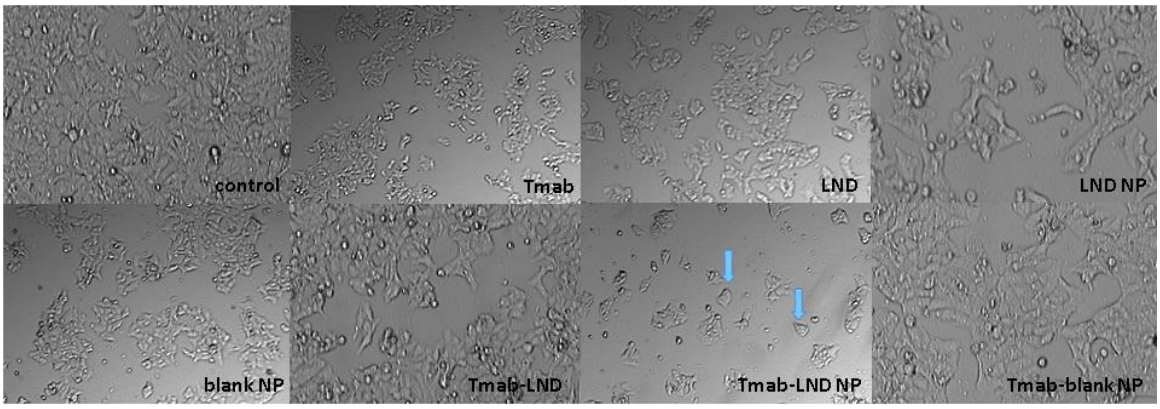


Figure 6.3.1. Microscope images of drug-treated cells

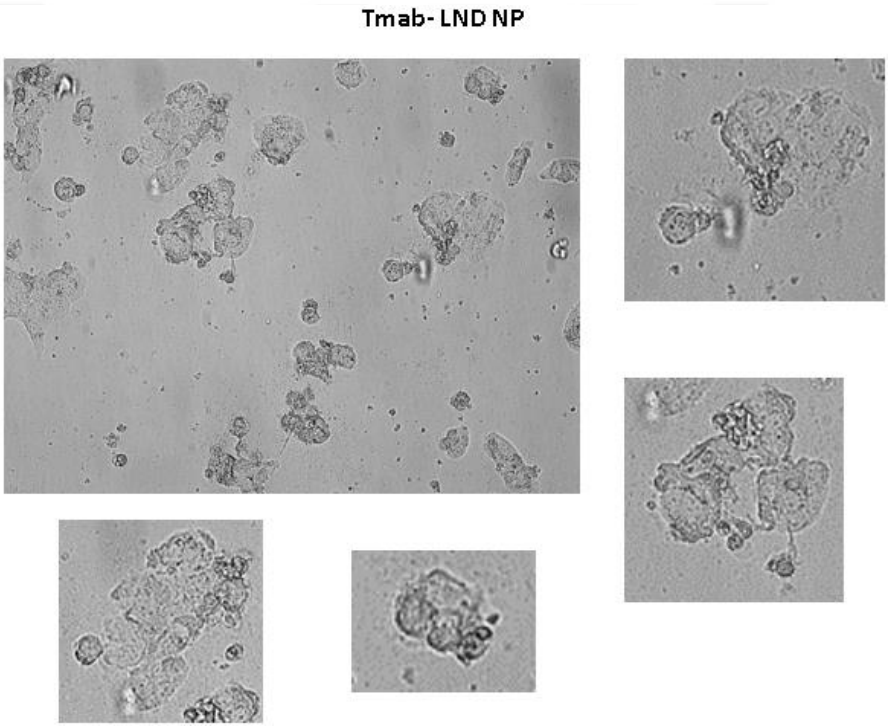


Figure 6.3.2. Tmab and LND NP combination treatment

6.4. Annexin V Results

The flow cytometry results, performed in duplicates, showed that among the drug treatments, LND-NP and Tmab combination had the highest effect on apoptosis induction after 48h incubation on SKBR3 cells ($p<0.0001$).

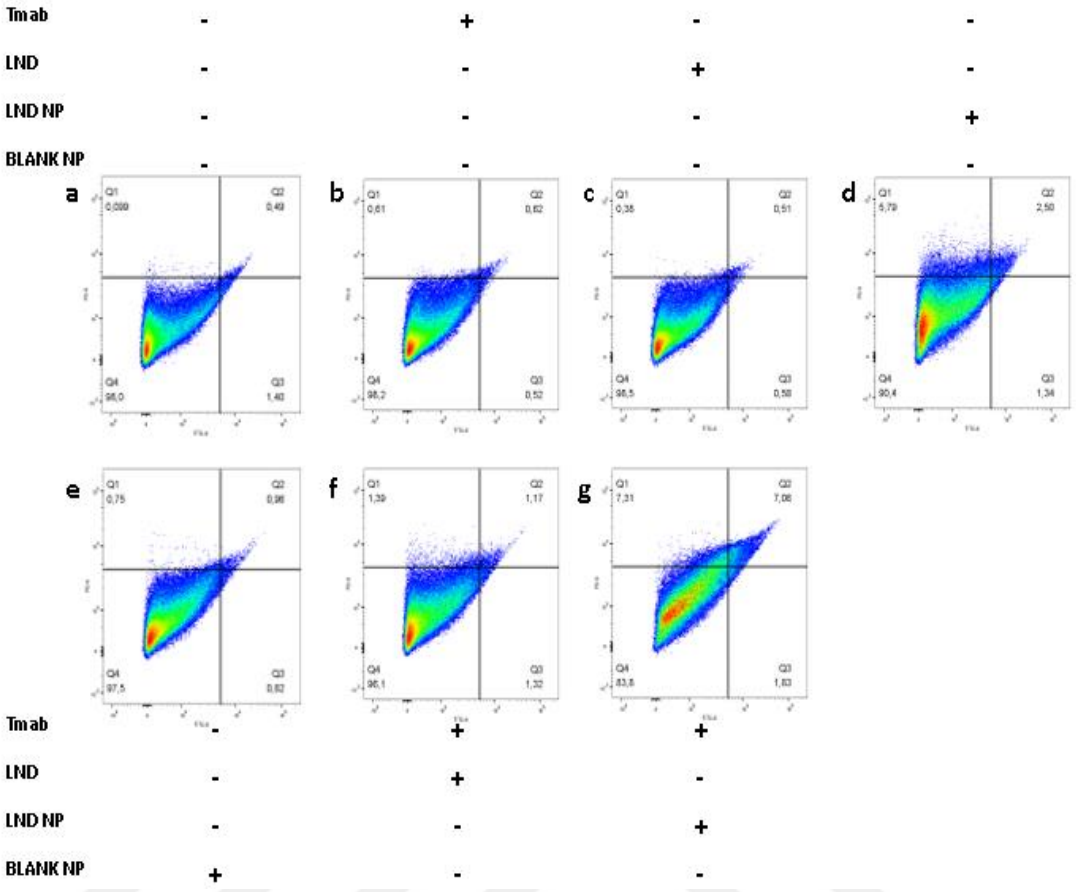


Figure 6.4.1. Flow cytometry analysis of cancer SKBR3 cells after 48h treatment with Lonidamine, Lonidamine-NP, blank-NP, trastuzumab and its combinations. Cells considered viable are Annexin V and PI negative.

When the Annexin V images were examined, the combination of LND-NP and Tmab expressed with g significantly led SKBR3 cells to apoptosis. The graphic below shows the statistical analysis of all groups and combinations.

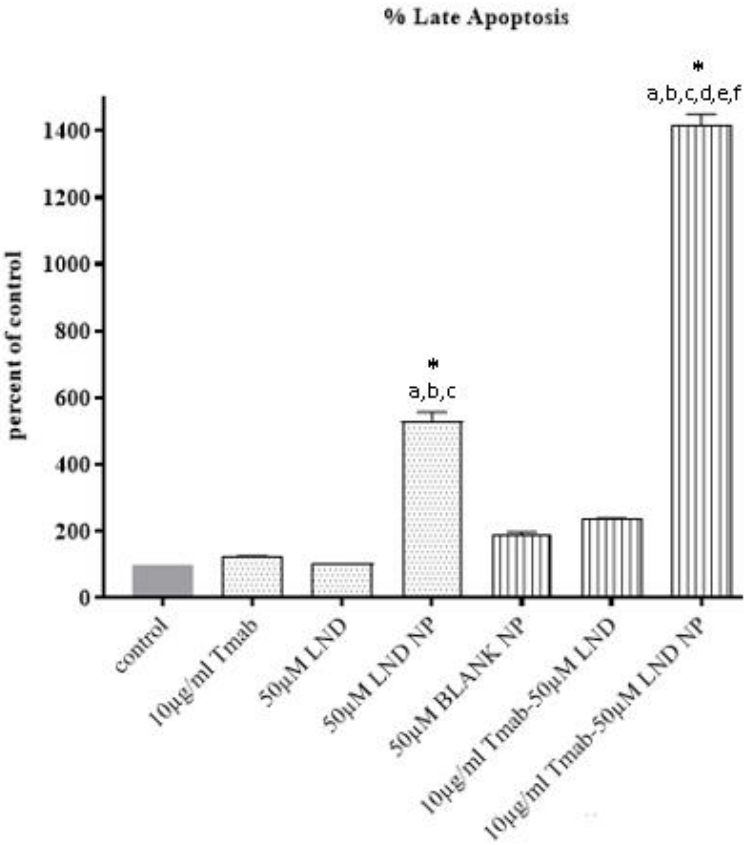


Figure 6.4.2. Statistical analysis of Annexin V results. The results were expressed as the mean of triplicates ± SD. Cells treated with control, LND (50 uM), LND-NP (50 uM), blank-NP(50 uM) and Tmab(10 ug/ml) (*$p < 0.0001$). *a significantly different from control, *b significantly different from Tmab, *c significantly different from LND, *d significantly different from 50 LND-NP, *e significantly different from blank-NP, *f significantly different from Tmab-LND combination.

Measurements of late apoptosis were calculated by proportioning them with the control group. According to this, control group 100 ± 0, Tmab group 125 ± 2,122, LND group 104,0±0,1131, LND-NP group 529,6±27,45, blank NP group 192,1 ± 5,433, Tmab-LND group 238,0 ±1,075, Tmab-LND NP group 1418±31,63 were calculated.

LND-NP significantly induced cells to apoptosis when compared between all doses and combinations. The combination of LND-NP and Tmab showed a synergistic effect. After 48 hours of drug exposure, the percentage of cells leading to late apoptosis and the percentage of dead cells increased significantly. In addition, empty nanoparticle structures encoded as Blank-NP showed a significant effect in cells.

6.5. Apoptotic DNA Ladder Kit Analysis

Apoptotic DNA fragmentation analysis was performed using the same doses and combinations as in the Annexin V experiments. Late apoptosis was observed in SKBR3 cells treated with the combination of LND-NP and Tmab, supporting the Annexin V results. The formation of a smear image in the cells treated with LND-NP and Tmab compared to the control and the brighter smear image compared to the other doses show that there is a correlation in both apoptosis experiments.

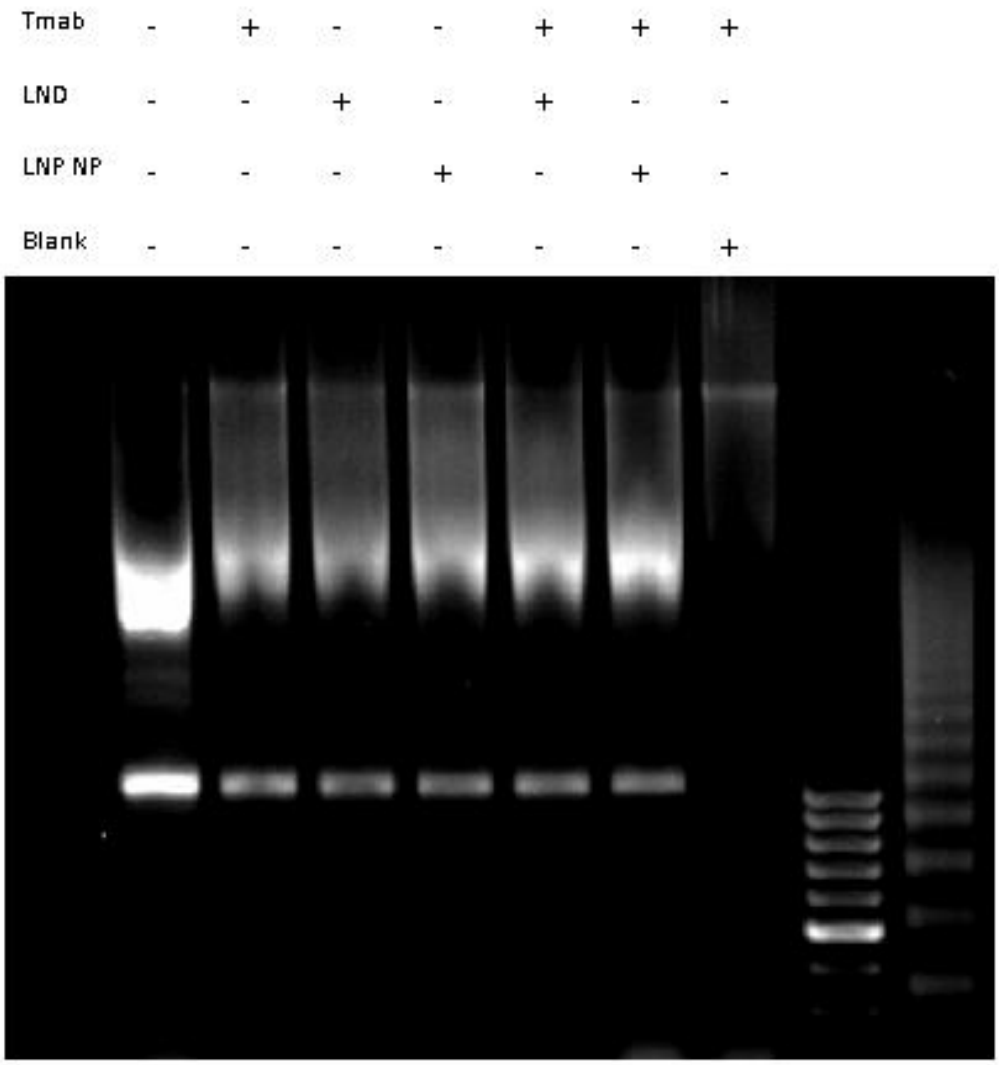


Figure 6.5.1. Analysis of apoptotic DNA fragmentation in SKBR3 cells after treatment.

6.6. Real Time PCR Analysis

Real-time PCR was used to assess the expression levels of BAX, BCL-2 and MMP-2 genes in breast cancer. In all assessments, untreated cells were used as negative controls. All the experiments were carried out in triplicates.

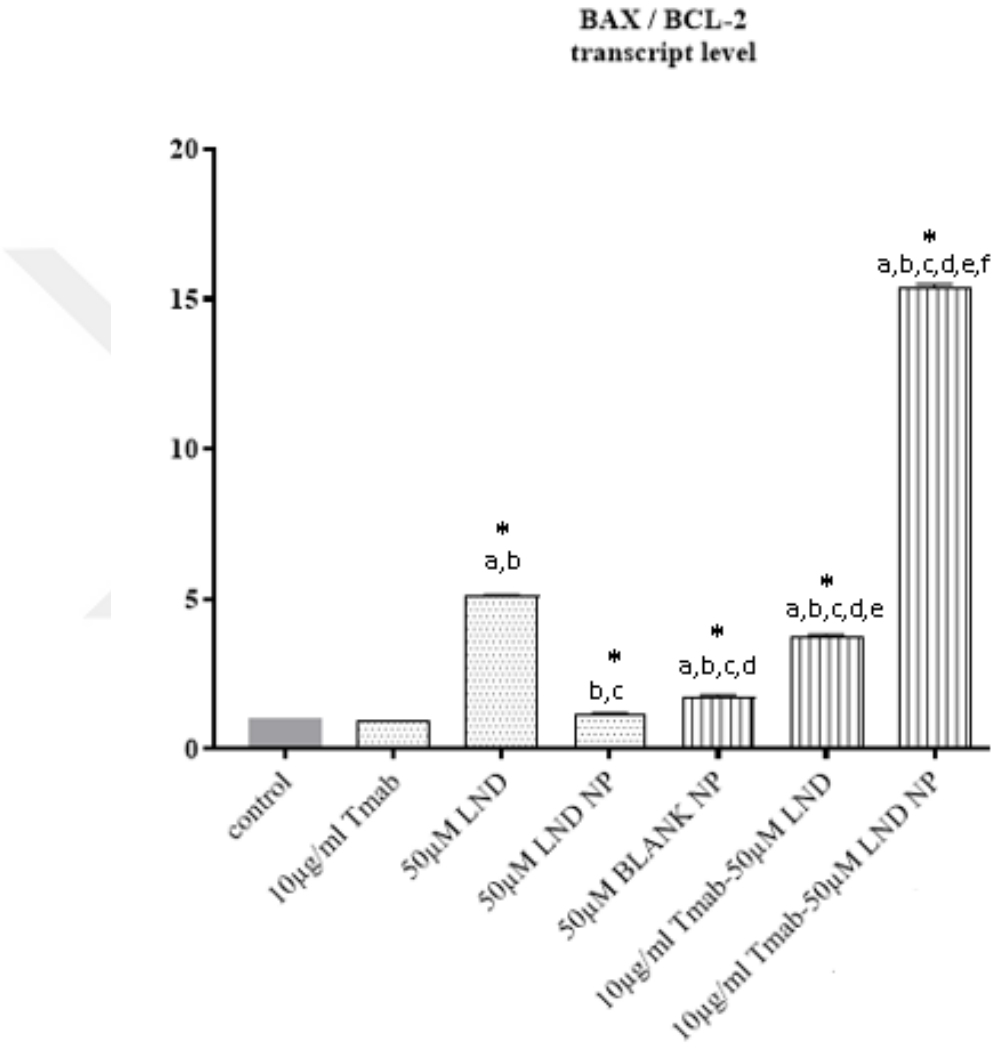


Figure 6.6.1. BAX/BCL-2 ratio. The results were expressed as the mean of triplicates ± SD. Cells treated with control, LND (50 uM), LND-NP (50 uM), blank-NP(50 uM) and Tmab(10 ug/ml) (*p < 0.0001). *a significantly different from control, *b significantly different from Tmab, *c significantly different from LND, *d significantly different from 50 LND-NP, *e significantly different from blank-NP, *f significantly different from Tmab-LND combination.

Measurements of BAX/BCL-2 ratio were calculated by proportioning them with the control group. According to this, control group 1 ± 0, Tmab group 0,9352 ± 0,006, LND group 5,123±0,010, LND-NP group 1,194±0,007, blank NP group 1,75 ± 0,07, Tmab-LND group 3,733 ±0,094, Tmab-LND NP group 15,37±0,1162 were calculated.

According to the Real-Time PCR results, the BAX/BCL-2 ratio was compatible with the other apoptosis data. Especially when only Tmab and LND NP are examined, there is a low rate, while the combination of the two drugs creates a synergistic effect and gives a significant BAX/BCL-2 ratio.

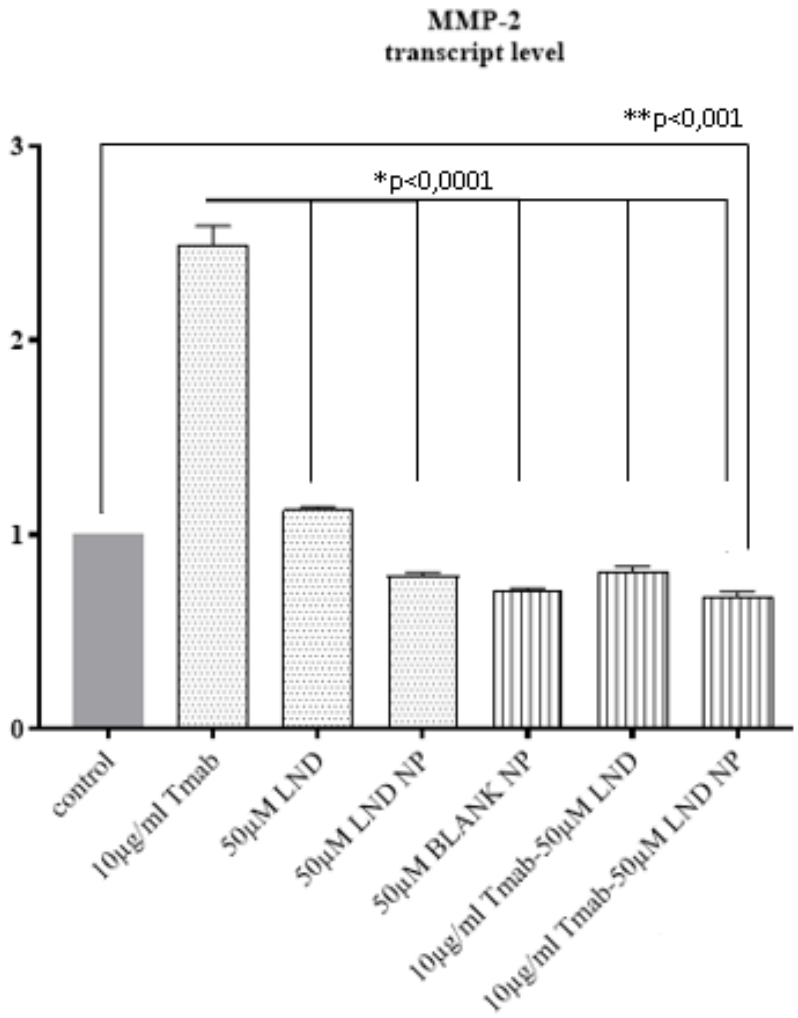


Figure 6.6.2. MMP-2 transcript level. The results were expressed as the mean of triplicates ± SD. Cells treated with control, LND (50 uM), LND-NP (50 uM), blank-NP(50 uM) and Tmab(10 ug/ml) (*p < 0.0001, **p<0,001).

Measurements of MMP-2 transcript level were calculated by proportioning them with the control group. According to this, control group 1 ± 0, Tmab group 2,490 ± 0,098, LND group 1.130±0,01414, LND-NP group 0,7900±0,01414, blank NP group 0,7100 ± 0,014, Tmab-LND group 0,8150 ±0,021, Tmab-LND NP group 0,68±0,028 were calculated.

The significant decrease in MMP-2 level in the Tmab-LND NP group compared to the control indicates that it will reduce the migration ability of cancer cells. The results are compatible with the scratch assay. In addition, treatment with trastuzumab alone increases MMP-2 levels, while combination with LND and LND NP causes significant decreases in MMP-2 levels.

6.7. Scratch Assay

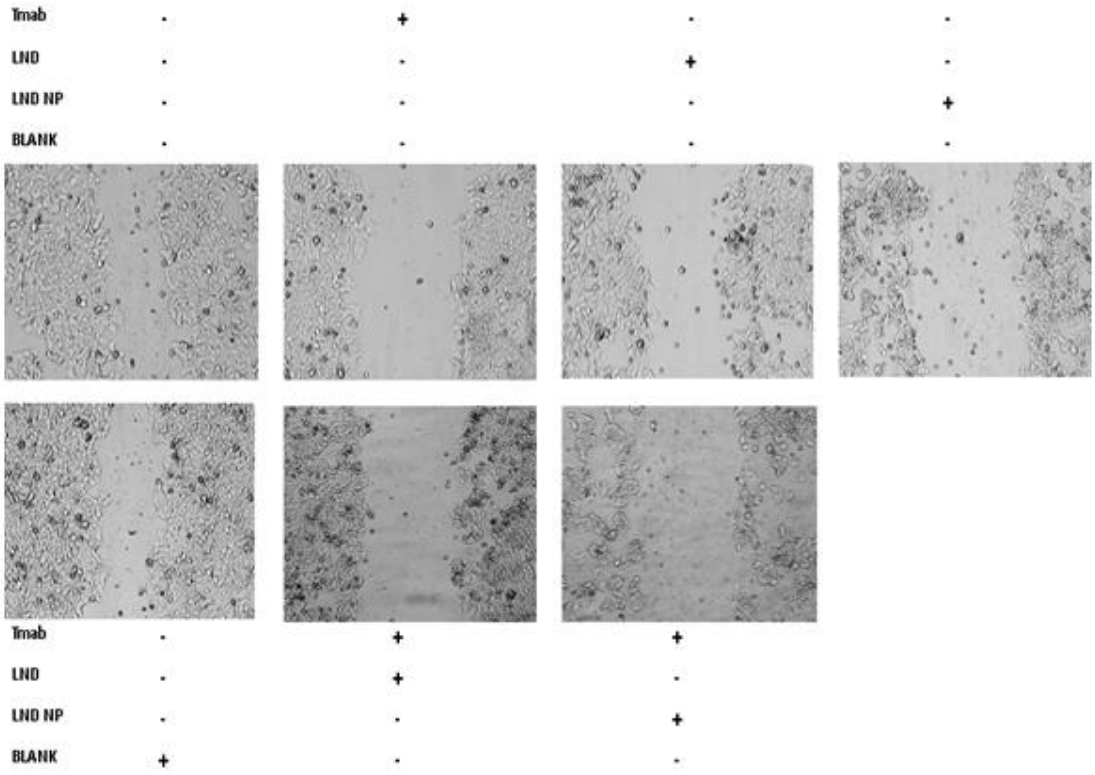


Figure 6.7.1. Scratch assay.

According to the Scratch Assay images and statistical evaluation, treatment with Tmab, LND and LND NP significantly inhibits the migration of cells. Combination groups significantly increase the wound area compared to drugs applied alone. In addition, the combination of Tmab and LND NP significantly increases the wound area compared to the combination in which Tmab and LND are applied together.

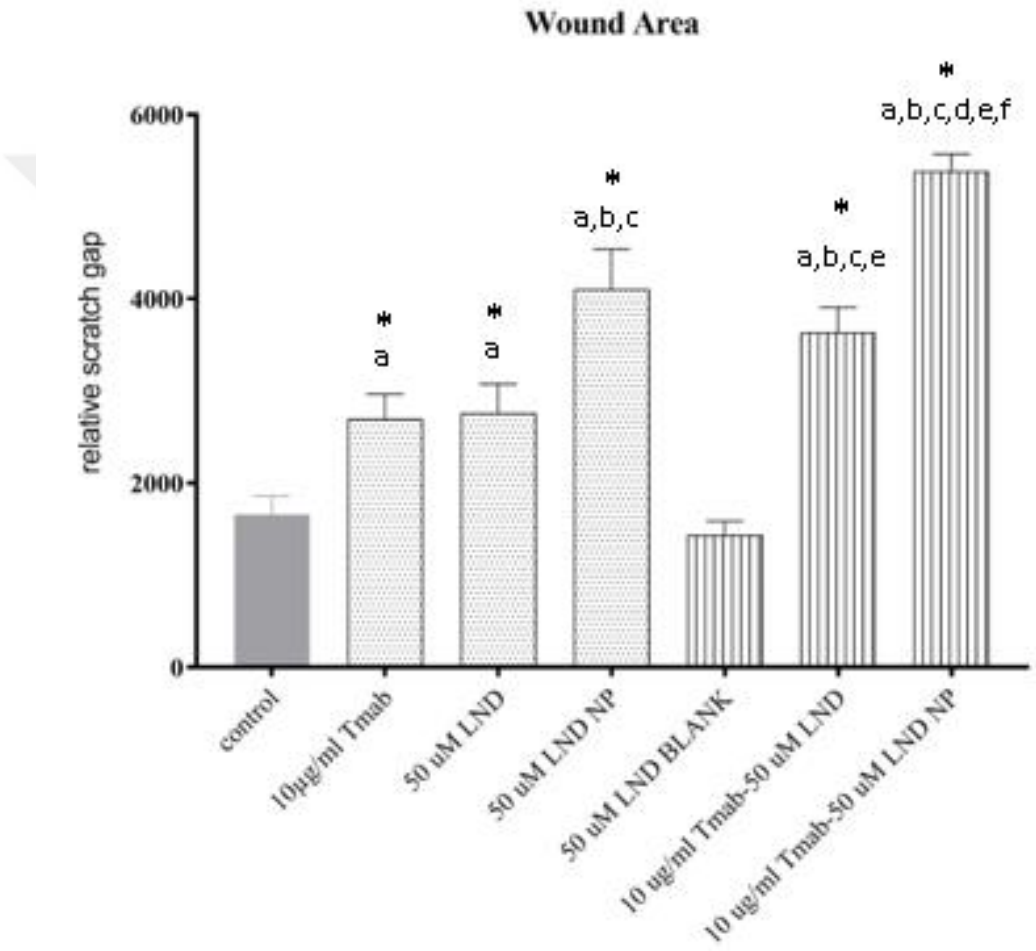


Figure 6.7.2. Statistical analysis of the scratch assay. The results were expressed as the mean of triplicates ± SD. Cells treated with control, LND (50 uM), LND-NP (50 uM), blank-NP(50 uM) and Tmab(10 ug/ml) (*$p < 0.0001$). *a significantly different from control, *b significantly different from Tmab, *c significantly different from LND, *d significantly different from 50 LND-NP, *e significantly different from blank-NP, *f significantly different from Tmab-LND combination.

Measurements of wound area were calculated by proportioning them with the control group. According to this, control group 1657 ± 204,6, Tmab group 2698 ± 268.1, LND group 2764 ± 311,4, LND-NP group 4100 ± 438,9, blank NP group 1438 ± 146,5, Tmab-LND group 3632 ± 276,6, Tmab-LND NP group 5386 ± 185,1 were calculated.

6.7.Western Blot Results

6.7.1. HER2 analysis

Trastuzumab was used as an inhibitor of HER2 overexpressed in SKBR3 breast cancer cell line. The aim of our study is to inhibit HER2 expression by the combination of lonidamine and trastuzumab. Based on the data obtained, the combination of Tmab and lonidamine appears to significantly reduce HER2 expression compared to cells exposed to lonidamine alone.

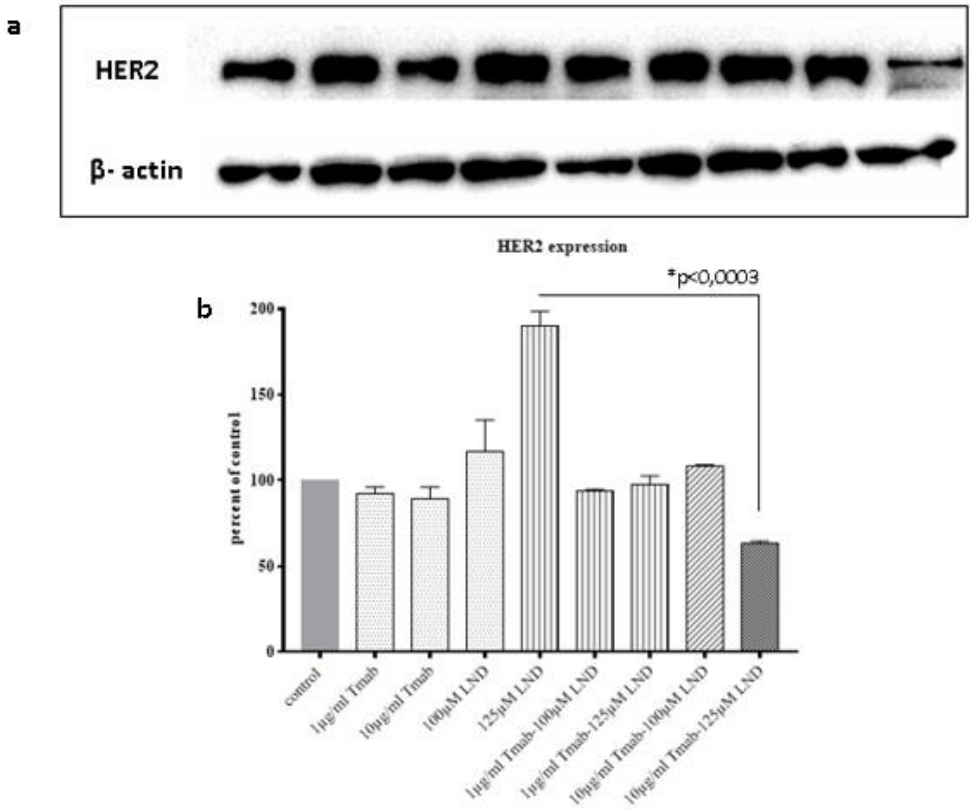


Figure 6.7.1.1. HER2 Analysis. The results were expressed as the mean of triplicates ± SD($p<0,0003$).

Measurements of HER2 expression were calculated by proportioning them with the control group. According to this, control group 100± 0, 1ug/ml Tmab group 92,29 ± 3,901, 10 ug/ml Tmab group 89,33 ± 6,802, 100uM LND group 116,9 ± 18,51, 125 uM LND group 190,5 ± 39,17, 1ug/ml Tmab-100uM LND group 93,74 ± 1,074, 1ug/ml Tmab-125uM LND group 97,77 ± 4,942, 10ug/ml Tmab-100uM LND group 109,2 ± 9,570, 10ug/ml Tmab-125uM LND group 63,30 ± 1,442 were calculated.

6.7.2. HK2 analysis

LND was used as HK2 inhibitor. Exposure to Tmab alone resulted in an insignificant increase in HK2 level, while the combination of LND with Tmab significantly decreased HK2 protein expression. The combination using IC50 doses caused a significant decrease in HK2 expression.

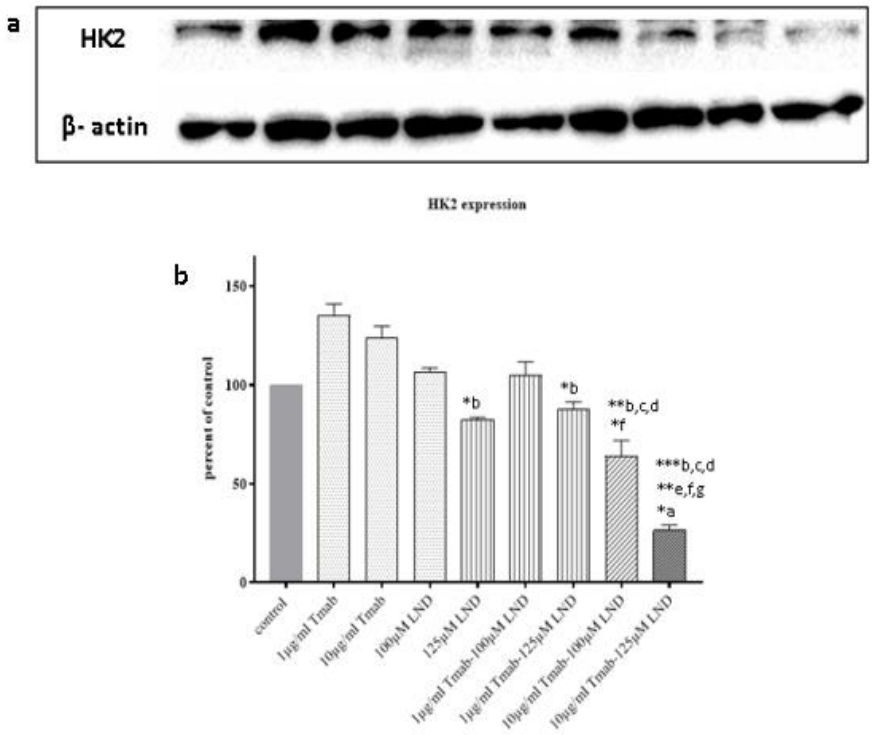


Figure 6.7.2.1. HK2 Analysis. a significantly different from control, b significantly different from 1 µg/ml Tmab, c significantly different from 10 µg/ml Tmab, d significantly different from 100 µM LND, e significantly different from125 µM LND, f significantly different from 1 µg/ml Tmab- 100 µM LND combination, g significantly different from 1 µg/ml Tmab- 125 µM LND combination, h significantly different from 10 µg/ml Tmab- 100 µM LND combination(*p<0,05, **p<0,005, ***p<0,0001).

Measurements of HK2 expression were calculated by proportioning them with the control group. According to this, control group 100± 0, 1ug/ml Tmab group 134,4 ± 18,53, 10 ug/ml Tmab group 124,0 ± 5,657, 100uM LND group 126,5± 2,121, 125 uM LND group 87,56 ± 3,175, 1ug/ml Tmab-100uM LND group 105,0± 13,80, 1ug/ml Tmab-125uM LND group 87,61 ± 7,939, 10ug/ml Tmab-100uM LND group 64,17 ± 16,28, 10ug/ml Tmab-125uM LND group 26,58 ± 2,598 were calculated.

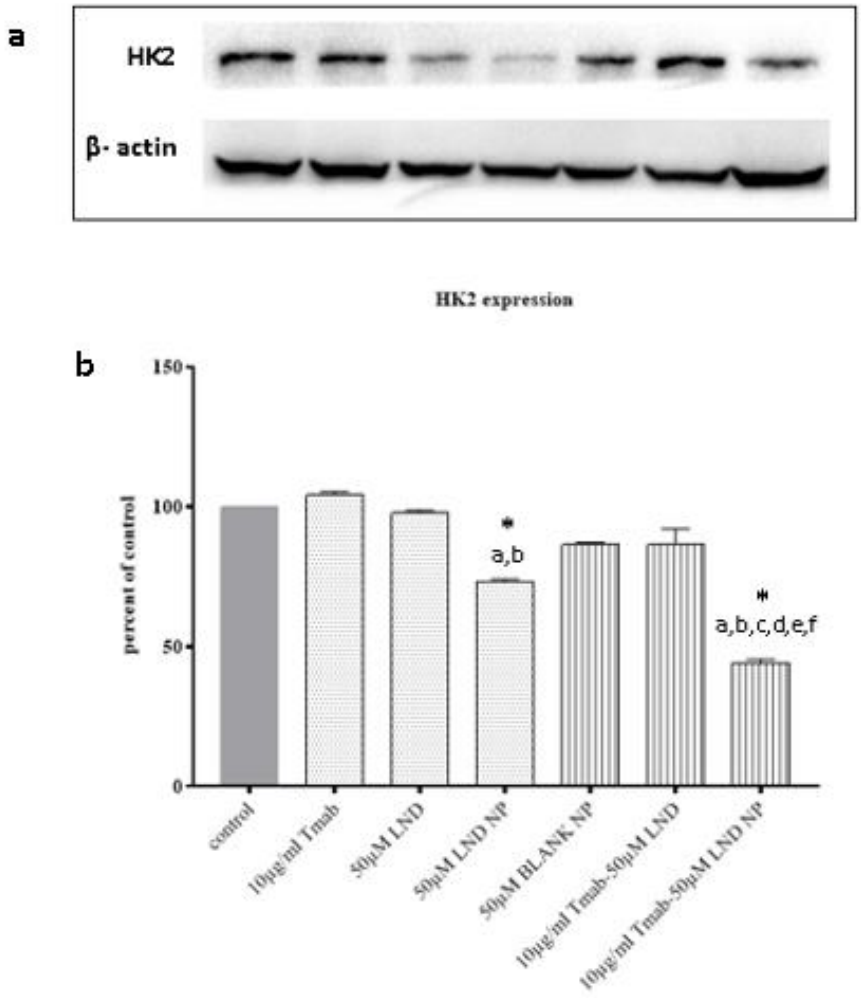


Figure 6.7.2.2. HK2 Analysis. a significantly different from control, b significantly different from 10 µg/ml Tmab, c significantly different from 50 µM LND, d significantly different from 50 µM LND NP, e significantly different from 50 µM BLANK NP, f significantly different from 10 µg/ml Tmab- 50 µM LND Npcombination($p<0,0001$).

Measurements of HK2 expression were calculated by proportioning them with the control group. According to this, control group 100± 0, 10 µg/ml Tmab group 104,3 ± 1,109, 50 µM LND group 97,88 ± 0,9093, 50 µM LND NP group 73,56± 0,6222, 50 µM BLANK NP group 86,67± 0,5124, 10 µg/ml Tmab-50µM LND group 86,66± 5,332, 10µg/ml Tmab-50µM LND NP group 44,22± 1,277 were calculated.

6.7.3. VDAC analysis

While VDAC protein expression increased at the LND dose exposed to the IC50 dose, the combination with Tmab had the opposite effect and decreased VDAC expression.

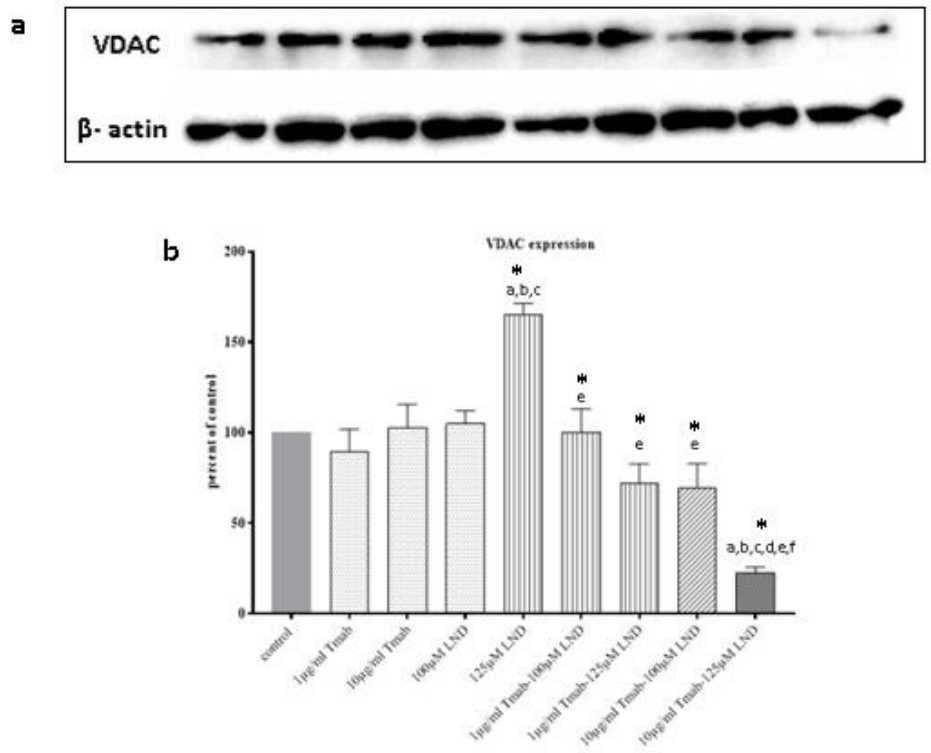


Figure 6.7.3.1. VDAC Analysis. a significantly different from control, b significantly different from 1 µg/ml Tmab, c significantly different from 10 µg/ml Tmab, d significantly different from 100 µM LND, e significantly different from125 µM LND, f significantly different from 1 µg/ml Tmab- 100 µM LND combination, g significantly different from 1 µg/ml Tmab- 125 µM LND combination, h significantly different from 10 µg/ml Tmab- 100 µM LND combination(*p<0,05).

Measurements of HK2 expression were calculated by proportioning them with the control group. According to this, control group 100± 0, 1ug/ml Tmab group 89,53± 12,24, 10 ug/ml Tmab group 102,9 ± 12,63, 100uM LND group 105,0± 7,071, 125 uM LND group 165,1 ± 6,341, 1ug/ml Tmab-100uM LND group 100,0± 13,00, 1ug/ml Tmab-125uM LND group 71,78 ± 10,92, 10ug/ml Tmab-100uM LND group 69,82 ± 13,09, 10ug/ml Tmab-125uM LND group 22,31 ± 3,378 were calculated(Fig 6.7.3.1).

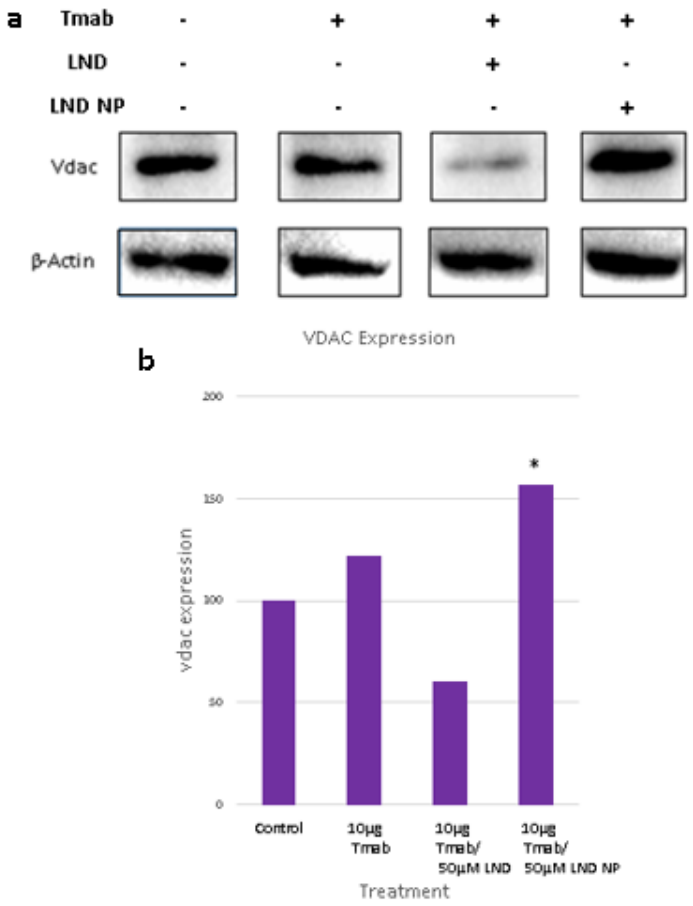


Figure 6.7.3.2. VDAC Analysis. Cells treated with control, LND (50 uM), LND-NP (50 uM),and Tmab(10 ug/ml) (*p < 0.005).

Exposure to LND alone increased VDAC expression, while combination with Tmab resulted in a significant decrease in VDAC expression. Thereupon, VDAC analysis was performed using Tmab-LND and Tmab-LND NP groups. As shown in Fig 6.7.3.2 the combination of LND NP and Tmab significantly increased VDAC expression with the opposite effect.

7. DISSCUSSION

Our study explains the targeting of two pathways and the effect of combined treatment in order to contribute to the chemotherapy process of HER2 positive breast cancer patients. As it is known, combined therapies can produce synergistic effects by targeting more than one pathway instead of a single target. It can also be useful in preventing drug-induced resistance by targeting both pathways. Recently, it has been seen that inhibiting the energy pathways of cancer cells gives successful results in cancer treatment. It has been determined that the glycolysis pathway, which is the first step of the energy production process, is over-activated in many cancer types. Another name for this effect is the Warburg Effect. In my thesis, we set the target to inhibit the glycolysis pathway by targeting the HK2 enzyme, which is associated with HER2 expression. The HER2 receptor protein, a tyrosine kinase protein, is overexpressed in some cancer cells. This results in increased survival, proliferation, and metastasis. In my thesis, we aimed to inhibit these two target pathways by using LND as HK2 enzyme inhibitor and Trastuzumab as HER2 receptor inhibitor and to observe the effectiveness on cell survival, apoptosis and proliferation. Although trastuzumab is currently used in chemotherapy, it shows drug resistance in long-term use. Although LND has been shown to be effective in clinical practice, its use is limited due to its toxic effects. By targeting these two pathways, it is expected that more than one death mechanism will be stimulated and a synergistic effect will occur.

Firstly, IC50 doses of Tmab, LND, and LND loaded hybrid NP were determined in SKBR3 cells. Since Tmab is an antibody and shows activity by binding to a receptor, long-term treatment is required. In this context, studies in the literature were generally carried out between 120h and 72h (85,98–102). LND and LND NP IC50 values were evaluated as 48h. According to the results obtained, Tmab 72h gave 9.5 µg/ml, Tmab 120h 1.12 µg/ml, LND 48h 125 µM and LND NP 45 µM IC50 values(Fig 6.2.1). The results of both Lonidamine and Tmab IC50 overlap with the literature studies (103–105). There is no LND and Tmab combination study in the literature. The images of cells exposed to drugs and combination doses are given in Figure.6.2.1. When the images are examined, it is seen that there is no change in cell morphology in general after 48h exposure with 10 µg/ml Tmab, while it inhibits cell proliferation in 50 µM

LND application. In addition, when the exposure of 50 μM LND loaded NP is examined, it is seen that both cell proliferation is inhibited and there are significant changes in cell morphology. In addition, an effective morphological change is observed in the combination of 10 μg/ml Tmab + 50 μM LND loaded NP. Accordingly, at 48h, the morphology of the cells completely changed and it was observed that apoptotic cell structures were formed (Fig 6.3.2). When apoptotic cells are examined in the literature, the images we have obtained are consistent with this information(106,107). In addition, our experiments for apoptosis explain the visuals.

The positron emission tomography (PET), which is used to observe the change in tumor tissue, is based on the inclusion of the marked isotope 2-[18F]-Fluoro-2-deoxy-D-glucose (FDG). In general, responsive tumors show a reduction in FDG uptake within a few days of starting chemotherapy compared to pretreatment. It has been shown that there is a decrease in FDG uptake after Trastuzumab in the treatment of HER2 breast cancer. Studies have revealed that inhibiting HER2 with Tmab also affects HK2. In the first study by Chenye RW et al., Tmab not only inhibited HER2, but also stated that this inhibition decreased the expression of HK2 and accordingly, FDG combination was also decreased(79). Later, Smith TA et al. demonstrated this effect with their xenograft model with mice. Tian C et al., is a new quinazoline derivative molecule with structural modification based on lapatinib named KU004. Studies have been done showing that this molecule is a HER2 inhibitor and later stated that this molecule is both a HER2 and HK2 inhibitor. As we mentioned above, HER2 inhibition also reduces HK2 expression(83,108). The formation of this effect may be due to the interaction of HER2 receptor and HK2 with each other via the AKT-PI3K pathway. In our study, the effects on cell growth and proliferation were investigated by inhibiting HER2 and HK2, whose expression is increased in cancer cells. In this context, according to Annexin V/PI analyzes after 48 hours of exposure, cell viability was 98% in control, 97% in 10 μg/ml Tmab and 50 μM LND, 90% cell viability and 2.5% late apoptosis in 50 μM LND loaded NP, In the combination of 10 μg/ml Tmab+50 μM LND loaded NP, cell viability was 83.8%, late apoptosis was 7.06% and dead cell percentage was 7.31%. According to these results, it is clearly seen that LND loaded hybrid NPs direct cells to apoptosis. In addition, the Tmab-LND loaded NP combination appears to be much more effective than the groups in which drugs are

administered alone, by creating a synergistic effect. There are studies showing that when LND and Tmab drugs are given as monotherapy, they cause cell death and even stimulate apoptosis(109–114). According to the apoptotic DNA fragmentation analysis performed in addition to Annexin V experiments, a higher rate of late apoptosis is observed in the 10 μg/ml Tmab+50 μM LND loaded NP combination group compared to the other groups. Late apoptosis was observed in the DNA fragmentation analysis in the 10 μg/ml Tmab+50 μM LND loaded NP combination group. Confirmation was made to be proportional to the broken DNA and high brightness was seen in Figure 6.4.1. Many mechanisms play a role in the formation of apoptosis. Proteins linked to the Bcl-2 family maintain the integrity of the mitochondria and are key regulators of mitochondria-initiated caspase activation. Some proteins belonging to this family can act as antiapoptotic (Bcl-2, Bcl-xl, etc.) and some proteins as proapoptotic (Bax, bak, etc.). The ratio between these antiapoptotic and proapoptotic members of the Bcl-2 family helps determine the sensitivity of cells to the death signal(115). Accordingly, the rate of change between them was analyzed by RT-PCR. Statistical analysis was performed by proportioning the gene expression levels (at the transcript level) of the proapoptotic gene BAX and the antiapoptotic gene BCL-2. BAX gene expression level increases in cells that will go to the apoptosis pathway, while BCL-2 gene expression level decreases(116–119). In our study, in comparison with the control, there was no significant increase in BAX/BCL2 ratio in the group given 10 μg/ml Tmab, but a significant increase in BAX/BCL2 ratio was observed in the 50 μM LND, 10 μg/ml Tmab+50 μM LND loaded NP and blank NP groups. The most significant increase was seen in the combination with 10 μg/ml Tmab + 50 μM LND loaded NP, which showed a 14-fold increase compared to the control. According to these results, induced apoptosis, was confirmed by Annexin V, Apoptotic DNA fragmentation analysis and RT-PCR results. In terms of the contribution of our study to the literature, induced apoptotic cells are formed with the combination of a targeted nanoparticle with Tmab and it gives a more effective result than the use of LND alone. In our study, all groups were used and each was compared with Tmab and LND NP.

Scratch assay analysis and MMP-2 gene expression analysis were performed to examine the effect of 10 μg/ml Tmab+50 μM LND loaded NP combination group on

metastasis. MMP-2 is known as matrix metalloproteinase-2 and gelatinase A(120). The MMP2 gene is located at position 12.2 on chromosome 16(121). This gene has been associated with metastasis. Studies based on MMP-2 gene inhibition in cancer cells are available in the literature (122–124). If the proliferation of cancer cells gets out of control, metastasis becomes inevitable. Wound healing (scratch assay) experiment is performed to observe metastasis in cancer cells(Fig 6.7.2). Accordingly, the closure of artificially created spaces over time is used to observe the effect of the applied treatment on metastasis. Accordingly, the gap area in the combination of 10 μg/ml Tmab + 50 μM LND loaded NP was found to be significant compared to all other groups in the experimental groups. It was observed that metastasis decreased significantly after this combination application. In addition, MMP-2 gene expression level was analyzed by Real Time PCR. When the MMP-2 gene expression level was examined, it showed a significant increase in the 10 μg/ml Tmab group. This increase is thought to be due to Tmab not reaching its effective duration. There was a significant decrease in MMP-2 gene expression level in the 10 μg/ml Tmab+50 μM LND loaded NP combination group compared to the control. This shows that the metastasis decreased proportionally with the wound healing experiment. In this context, it can be said that the combination used inhibits the metastasis of cancer cells.

HER2, HK2, and VDAC protein levels were analyzed by the Western Blot Method. The binding of HK2 to VDAC puts pressure on VDAC and apoptosis is suppressed. Inhibition of HK2 reduces HK2 binding on the VDAC, thereby inhibiting apoptosis suppression(75). According to Western blot analyses to observe this mechanism, treatment with Tmab alone causes an increase in HK2 protein level while decreasing HER2 protein level. However, the combination of Tmab and LND applied at IC50 doses significantly reduces HK2 expression. The synergistic display of the effect of LND with Tmab was seen at the HK2 protein level (Fig 6.8.2.1). Afterward, VDAC protein expression analysis was performed. According to VDAC analysis, VDAC expression shows a significant decrease in the combination of Tmab and LND (Fig 6.8.3.1).With the decrease of HK2 expression, it was expected to increase VDAC expression with the opposite effect. However, the opposite result was obtained. Afterward, VDAC analysis was performed with the combination of 10 μg/ml Tmab + 50 μM LND loaded NP, and the combination of Tmab and LND was compared.

According to this experiment, a significant increase in VDAC protein expression was observed, as expected(Fig 6.8.3.2)(125,126). By blocking the HK2, the pressure on the VDAC can be eliminated. As a result, apoptosis is induced. VDAC is a class of porin ion channels located on the outer mitochondrial membrane. Accordingly, the detachment of HK-2 from VDAC causes disruption of BCL-XL-BAX interaction and release of BCL-XL. The release of BCL-XL facilitates BAX binding, which prevents BAX-BAK interaction and protects against OMM permeation. It forms pore structures that allow released BAX to interact with BAK and promote the release of cytochrome-c and other apoptosis proteins in the outer membrane. This leads to the initiation of apoptosis (75). As a result, intrinsic apoptosis occurs.

Discussion on lonidamine-loaded liposome-based hybrid nanoparticle formulations

The encapsulation efficiency values of liposome-based hybrid nanoparticle formulations loaded with lonidamine were determined in a narrow range of 81.47% - 93.89%. The encapsulation efficiency values of the prepared formulations increased statistically as the particle sizes of the nanoparticles increased ($p<0.05$). This situation was realized by the increase in the viscosity of this phase due to the increase in the ratio of active substance in the organic phase, and thus the higher level of lonidamine loading on the nanoparticles due to the increase in the particle size of the nanoparticles(127,128) (Table 6.1.1.1).

When the particle size values of liposome-loaded hybrid nanoparticle formulations containing lonidamine in different ratios (5-10% and 20% of the polymer) are examined in terms of formulations containing and without active ingredient, the particle sizes of formulations containing lonidamine are primarily determined in the range of 160.1 nm to 201.4 nm ($p <0.05$) The particle size of the empty nanoparticle formulation without lonidamine was determined as 147.8 nm. It was determined that the particle sizes of the formulations containing lonidamine increased statistically significantly depending on the increase in the active substance content. It is thought that this is due to the increase in the viscosity of the organic phase, resulting in the formation of a more viscous organic phase that is more difficult to disperse in the water

phase during sonication, and it has been determined that an increase in particle size is observed in this way(128,129). The particle size of the empty formulation without lonidamine was determined as 147.8 nm and it was determined that there was a statistically significant reduction in the particle size due to the fact that the active ingredient was not included in the formulation content ($p>0.05$) (Table 6.1.1.1).

When the PDI values of the developed liposome-based hybrid nanoparticle formulations were examined, it was determined that the particle size distributions were determined in a narrow range on the basis of all the formulations prepared ($PDI<0.2$) (Table 6.1.1.1)(128).

When the determined zeta potential values of the prepared liposome-based hybrid nanoparticle formulations were examined, it was determined that the nanoparticles had a negative surface charge in the range of -28.9 mV to -31.7 mV. It was determined that the presence of lonidamine and the investigated active ingredient ratios did not have any effect on the zeta potential values of the nanoparticles ($p>0.05$) (Table 6.1.1.1).

It was determined that the liposome-based hybrid nanoparticle formulations prepared within the scope of the thesis study could be obtained in a spherical shape and it was determined that the phospholipid shell wall of the nanoparticles could be observed clearly (Fig 6.1.2.1).

When the release rate of lonidamine from the developed liposome-based hybrid nanoparticles was evaluated over the active substance ratio, it was determined that the release profiles were proportional to the varying particle sizes ($p<0.05$). As a result of in-vitro release rate studies carried out for 22 days, it was observed that approximately 55.27% - 83.21% of lonidamine was released from the formulations developed. During this period, the highest release of active substance from the liposome-based hybrid nanoparticle systems was achieved in the DF1 coded formulation.

8. CONCLUSION

Our study includes targeted inhibition of glycolysis of the HK2 enzyme and targeted inhibition of the overexpressed HER2 pathway. With the combined inhibition of these two targets, low survival, negative metastasis and induced apoptosis are expected to be observed. The combination of LND loaded hybrid NP and Tmab developed for this purpose showed a synergistic effect. In this context, it has been shown by different molecular experiments that the combination of 10 μg/ml Tmab + 50 μM LND loaded NP induced apoptosis. When all parameters were examined, the combination of 10 μg/ml Tmab + 50 μM LND loaded NP showed increased apoptosis. Our study presents the molecular mechanisms that Tmab, which is an effective drug in breast cancer, and LND loaded hybrid NPs can be an effective combination therapy in chemotherapy. Our study needs to be supported by in vivo experiments and efficacy studies are needed. If the results of these experiments are promising, an important chemotherapy opportunity may be offered for HER2 positive cancer patients.